Pulsed Laser Patterning of Toric Contact Lens Inserts

By

Avinash Parashar

A Thesis

In

The department

Of

Mechanical and Industrial Engineering

Presented in partial fulfillment of the requirement

For the Degree of Master of Applied Science (Mechanical Engineering)

at

Concordia University

Montreal, Quebec, Canada

July, 2008

Your file Votre référence
ISBN: 978-0-494-42524-4
Our file Notre référence
ISBN: 978-0-494-42524-4

ABSTRACT

Pulsed Laser Patterning of Toric Contact Lens Inserts

Avinash Parashar

Laser patterning is a promising technology for biomedical applications. In this research project, a novel laser based marking method for toric contact eye lenses has been proposed. Toric contact eye lenses are designed to address general blurring that occurs due to uneven cornea which is known as astigmatism. Toric lenses have two powers in them, created with curvatures at different angles of cone. For proper functioning of toric lenses their orientation with respect to eye is critical. So toric lenses are manufactured with some form of marking which helps in deciding the orientation with respect to eye. The proposed method is to use the principle of laser interferometry in marking the metal inserts which will subsequently be transferred to lens surface during injection molding.

For the research project stainless steel was selected as the material from the commonly used materials for the lens inserts. The marking of stainless steel with respect to different laser parameters (e.g. peak pulse power, rep rate, polarization and marking time) was studied. Mathematical modeling has also been done to predict the effect of aspherical curvature of lens insert on marking parameters and to study the effect of laser interference on the marking quality and quantity of stainless steel. The proposed marking method will not only reduce the marking area on the toric lens but also increase the visibility of the marking. In addition, using the principle of interference in marking reduces the amount of laser energy required for marking which reduces the heat affected zone thereby increasing the life of high value added metal inserts.

Acknowledgement

I would like to thank my thanks my supervisor Dr. Narayanswamy Sivakumar for the valuable guidance, patience and support that he provided throughout the course of my graduate thesis work.

I would like to thank Mr. Eric from Polytechnic Montreal, who provided me support related to surface characterization of machine samples. Also I like to thank my colleagues at the Optical Metrology lab Ankur Shah and Jasjit Singh Mann, whose ideas and support and help make this work possible.

Finally I would like to express my deep gratitude to my parents, brother and my wife for their ever support and encouragement. They have always been a source of inspiration for me.

Table of Contents

List of Figures.....ix

List of Tables.....xii

Chapter 1 Introduction

1.1 Introduction..... 1

1.2 Contact Eye Lens..... 2

1.3 Manufacturing of Contact eye lens..... 2

1.4 Contact eye lenses can be divided broadly into these categories..... 4

1.5 Orientation of toric contact lenses..... 5

1.6 Contact eye lens marking methods proposed in the past research..... 6

1.6.1 Region of marking of contact eye lens..... 6

1.6.2 Dimensions for the marking..... 8

1.6.3 Marking Methods of contact eye lenses..... 9

1.6.4 Marking with laser..... 10

1.6.5 Marking with ultra fast laser inside the lens..... 11

1.6.6 Marking of metal mold inserts with laser beam..... 11

1.7 Introduction to Lasers..... 12

1.7.1 Laser Properties..... 13

1.7.2 Laser types..... 14

1.8 Pulsed Laser Surface micromachining..... 15

1.8.1 Femto second pulse micro patterning..... 15

1.8.2 Pico second pulse micro patterning..... 16

1.8.3 Nano second pulse micro patterning 16

1.9 Laser Processing Parameters 17

1.10 Interferometry 18

1.10.1 Two Beam Interferometry 19

1.10.2 Interference in micromachining 20

1.10.3 Common types of interferometers used for micromachining 20

1.11 Definition of the Problem 24

1.12 Objective of the work 25

1.13 Scope of work 26

1.14 Summary 27

Chapter 2 Theoretical Modeling

2.1 Introduction 28

2.2 Asphericity of the male insert 28

2.2.1 3D profile of the Contact lens Surface 31

2.3 Effect of asphericity on marking depth 32

2.4 Intensity distribution with or without interference 34

2.5 Machining with different laser power 37

2.6 Depth of Machining with laser power 39

2.7 Depth of machining with repetition rate 41

2.8 Variation of pitch of patterns 43

2.9 Summary 44

Chapter 3 Experimental Setup

3.1 Introduction 45

3.2 Explanation of the setup 45

3.3 Details of laser optics used in experimental set up 47

3.3.1 Nd: YVO4 Laser 47

3.3.2 Wave Plate 48

3.3.3 Wollaston Prism 51

3.3.4 Cylindrical Plano Convex Lens 51

3.4 Optical Setup description 52

3.4.1 Laser Beam Alignment 53

3.4.2 Alignment of first Wollaston prism 53

3.4.3 Alignment of next two Wollaston prisms 55

3.4.4 Alignment of the half wave plate 55

3.4.5 Alignment of the distance between the two out put beams 56

3.5 Transmission efficiency of common optics 57

3.6 Refinements 58

3.7 Summary 60

Chapter 4 Optimization of Laser Parameters

4.1 Introduction 61

4.2 Influence of laser power 61

4.3 Effect of repetition rates 69

4.4 Variation in depth with different variation in number of pulses 74

4.5 Summary 79

Chapter 5 Optimization of Setup Parameters

5.1 Introduction 80

5.2 Variation in the pitch of the fringe patterns 80

5.2.1 Variation in pitch with different beam spacing 81

5.2.2 Variation in pitch with different focusing lens 83

5.3 Number of fringe patterns machined 87

5.4 Machining with different set of laser polarization 89

5.5 Summary 93

Chapter 6 Conclusion

6.1 Conclusion 94

6.2 Future Work 96

Reference 97

Appendix 1

Average Laser Pulse Power

Appendix 2

Experimental Details

Appendix 3

MATLAB Coding

List of Figures

1.1 Metal Mold inserts pair for casting thermoplastic cups.....3

1.2 Step by step method for manufacturing contact eye lens.....3

1.3 Different type of toric lens marking.....5

1.4 Different regions of lens corresponds to the respective eye position.....7

1.5 Width vs. Depth of marking.....9

1.6 Different zones of the color used for the marking on the lens surface.....9

1.7 Mask for the laser marking.....12

1.8 Marking done at the outer periphery of the contact lens.....12

1.9 Schematic view of laser mechanism.....13

1.10 Adopted Mach- Zehender Interferometer.....21

1.11 Interferometer machining setup.....22

1.12 Three mirror interferometer.....23

1.13 Optical setup..... 24

1.14 Number of grating lines machined within focused spot size.....26

1.15 Proposed Marking method.....26

2.1 Affect of asphericity on contact lens surface.....30

2.2 Marking region on the modeled toric lens insert.....31

2.3 3D profile of contact lens insert.....32

2.4 Variation Curve of Machining Depth Due to Curvature of Lens Insert.....33

2.5 Variation Curve of Machining Depth Due to Curvature of Lens Insert 34

2.6 Intensity distribution curve.....36

2.7 Machined size of patterns at lower peak pulse power 38

2.8 Machined size of patterns at higher peak pulse power 38

2.9 Depth of machining with different laser power.....40

2.10 Depth of machining with different rep rate 41

2.11 Pitch variation with focusing angle 44

3.1 Machining setup.....46

3.2 Waveplate.....48

3.3 Working principle of quarter waveplate..... 49

3.4 Working principle of half waveplate.....50

3.5 Wollaston prism.....51

3.6 Cylindrical lens.....52

3.7 Laser beam alignment.....53

3.8 Wollaston alignment.....54

3.9 Alignment of focusing optics.....57

3.10 SEM image for out of plane focusing.....59

3.11 SEM image for in plane different focusing spot.....59

3.12 Machined spot with all refinements.....60

4.1 SEM images for machining with different laser peak pulse power.....63

4.2 Comparison of experimental vs. theoretical values 64

4.3 SEM images for different regions of same spot 66

4.4 Microscopic images of depth characterization with different peak pulse power.....67

4.5 Experimental Values of depth with respect to different peak pulse power.....68

4.6 SEM images of machined patterns at different rep rates.....69

4.7 Microscopic images for spots machined with different rep rate.....73

4.8 Comparison of experimental and theoretical values for different rep rates.....74

4.9 Microscopic images of depth characterization with number of pulses.....76

4.10 Experimental values for the depth of machining.....76

4.11 SEM images for different machining time.....78

5.1 Focusing angle theta with Z and F.....80

5.2 SEM images for patterns machined with different beam spacing.....82

5.3 Comparison of experimental and theoretical values for different pitch.....83

5.4 SEM images for different focusing lens machining for pitch.....85

5.5 Comparison of experimental and theoretical values for different focusing lens.....86

5.6 Comparison of theoretical and experiments results.....87

5.7 Comparison of theoretical and experiments results.....88

5.8 Experimental setup for one state of polarization.....90

5.9 SEM image for one set of polarization.....91

5.10 Experimental setup for another state of polarization.....92

5.11 SEM image for another set of polarization.....92

LIST OF TABLES

3.1 Transmission efficiency of optics used in the machining setup.....58

4.1 Comparison of experimental Values with the theoretical for focused width.....64

4.2 Comparison of experimental values with theoretical for focused width.....73

5.1 Comparison of experimental pitch with theoretical pitch for different beam spacing.....82

5.2 Experimental and theoretical values for pitch with different focusing length.....86

5.3 Number of fringe patterns with different average pulse power.....87

5.4 Number of fringe patterns with different rep rate.....88

Chapter 1

Introduction

1.1 Introduction

Concept of contact lens came first time into existence in 1880 due to independent contribution of Adolf E. Fick, Eugene Kalt and August Muller besides these scientists Leonardo Da Vinci is also considered as one who describes the concept of contact eye lenses in his sketches [1, 2]. These scientists produced glass sclera shells as contact eye lenses. All these scientists designate his invention with a different name, Fick called "Contactbrille", Muller called "Hornhautlinsen". Kalt was the first scientist who treats Keratokonus with glass shell having diameter equal to the cornea of the human eye [3].

Soft contact lenses was first introduced in 1970, whereas the first toric contact ye lens for the correction of astigmatism was developed in 1977.Contact eye lenses are marked for identification of up and down side, right and left, maintaining inventory and for deciding orientation axis of lens with respect to eye in case of toric contact lenses. With the advent of new laser micromachining techniques the marking of the contact eye lens become simpler and straightforward. Laser marking is a rapid, non-contact means of producing permanent high resolution images on the surface of most engineering material. Laser marking is a clean process no paints, inks or acids are used, which could contaminate the product. This also avoids the need to dispose of toxic solvents. There is

no material distortion and no tool wear since it is a non- contact process involving low levels of power.

For the last two decades different marking methods have been proposed by the researchers and majority of them are based on the laser micromachining. Pulsed laser has changed the whole scenario by decreasing the heat affected zone and better control of the laser energy. With the application of the interference in micromachining the machining of sub spot size dimensions is quite easier and straightforward. The application of such a selective micromachining with laser Interferometry technique is proposed for marking of the toric contact eye lenses in this research project.

1.2 Contact Eye Lens

A contact eye lens as name suggests is the lens which is kept in direct contact with the cornea of the eye. Modern contact lenses were invented by the Czech chemist Otto Wichterle, who also invented the first gel used for their production. Contact lenses usually serve the same corrective purpose as convention glasses, but are lightweight and virtually invisible.

1.3 Manufacturing of Contact eye lens

Contact eye lenses are manufactured by the injection molding process as shown in fig.1.2. Initially metal mold inserts (shown in fig.1.1) are used for manufacturing

thermoplastic casting cups. These thermoplastics mold will be used only once to cast a single contact lens [5]. Some of the common metals described in literature for metal inserts are copper, stainless steel and brass. Thermoplastic casting cups produced by metal inserts basically made up of any of these polymers e.g. polystyrene, poly ethylene and polypropylene [6]. Hydro gels are the most common material for casting contact eye lenses from thermoplastic molds. Hydro gels normally contain more then 80 % of water [7].

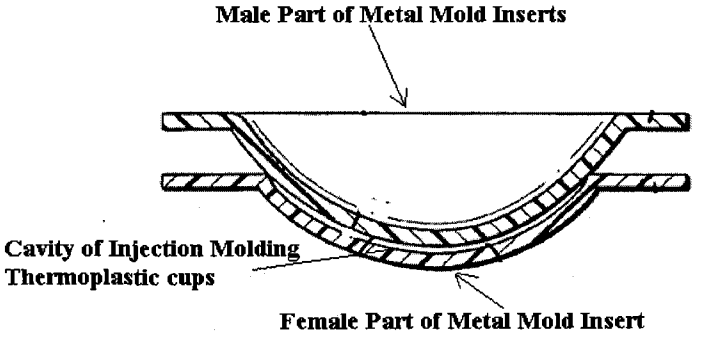

Fig.1.1 Metal Mold inserts pair for casting thermoplastic cups [4]

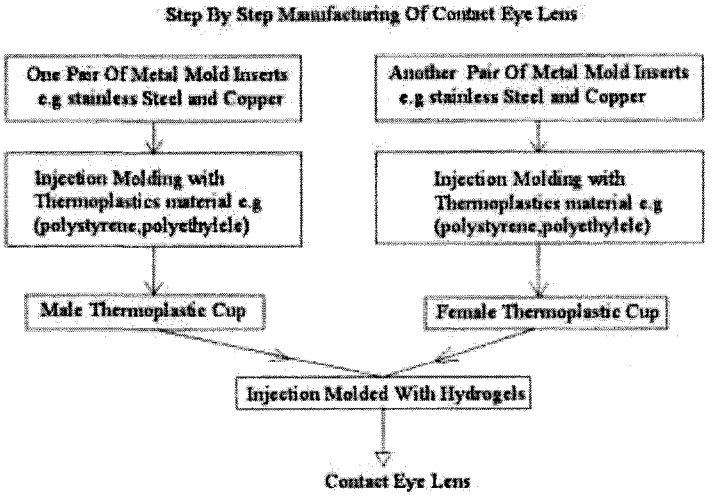

Fig.1.2 Step by step method for manufacturing contact eye lens

1.4 Contact eye lenses can be divided broadly into these categories

Contact eye lens can be broadly divided into two main categories on the basis of their shapes. Most of the contact lens belongs to first and most common category of contact eye lenses known as spherical contact eye lens. Spherical contact eye lenses are used either for correcting eye sight or for decorative purposes (changing color of the eye) [8]. Second type of contact eye lenses is known as toric contact lenses, these toric lenses are not as common as spherical contact lenses. Difference in spherical and toric lenses is in it's functionally due to the difference in their design and shape. Toric contact eye lenses are designed to address general blurring that can occur usually due to the uneven shape of the cornea which is known as astigmatism. Toric lenses have two powers in them, created with curvatures at different angles of cone, one for astigmatism and the other for correcting eye sight.

For proper functioning of toric contact eye lens their orientation with respect to eye is very critical, which makes toric contact lenses a special purpose lens. Toric contact lens can be made from rigid or soft material. Currently rigid toric lenses which are generally made up of PMMA are now out dated and soft hydro gels are common material for toric lenses. Due to low modulus of elasticity of hydro gels these toric contact eye lens rotates on the eye, whereas for proper functioning of toric lenses their orientation with respect to eye is very critical [9,10].

1.5 Orientation of toric contact lenses

Soft toric lenses are manufactured with some form of marking which helps in deciding the orientation of the toric contact eye lens with respect to eye. This is carried out with the help of slit lamps. If the lens rotates more then 30° from its correct or specified position then there is inadequate stabilization and an alternative toric lens design is considered [10].

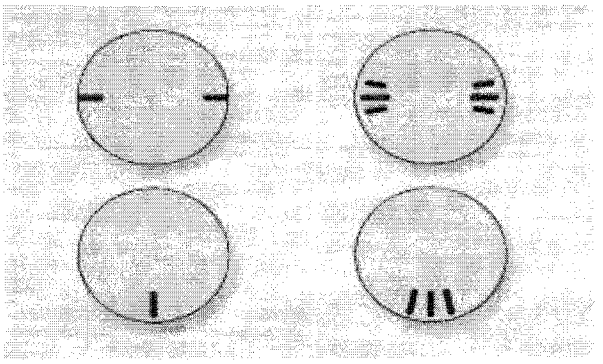

Fig.1.3 Different type of toric lens marking [11]

Most common types of marking used with toric contact eye lenses are shown in fig.1.3. In fig. 1.3 the left lens on the top shows the marking done only for one axis whereas in the right lens next to it besides marking, rotation marks were also made which helps in deciding the rotation of the lens with each eye blink.

It is important to know that the exact configuration or shape of the marking is not critical so long as the marking is indicative of an offset between the toric lens axis and the eye [12-15].

1.6 Contact eye lens marking methods proposed in the past research

For the last few years many contact lens marking methods have been proposed and some of them are also registered as patents. Mainly marking of the contact eye lenses can be classified in two different sections.

(a) Direct Marking on the Contact eye lens:

In this method of marking is done directly on the contact eye lens. Direct marking of contact eye lenses are time consuming and not feasible or adaptable with ever increasing production demands [5, 20, 21].

(b) Indirect Marking on the contact eye lens

In this method of marking recessed marks are created on metal mold inserts, hence the thermoplastic molding cups have raised portion in the region corresponds to metal insert marking and this marks will be subsequently transferred on the contact eye lens in further molding process [5].

1.6.1 Region of marking of contact eye lens

The area of the contact lens can be divided as shown in the fig.1.4, where each region corresponds to the respective position on the eye. In the figure the inner region marked as 'A' corresponding to the pupil of the eye with radius of curvature R1

approximately equal to 2.5mm. This area is critical for the transmission of the light to the pupil of the eye for the proper visibility, so cannot be used for any marking purposes. Region surrounding 'A' region (pupil of the eye) is known as iris. Iris can be divided into two regions, inner region marked as 'B' with radius of curvature (R2) 3.5mm and out region marked as 'C' with radius of curvature (R3) approximately 5mm as shown in fig.1.4 respectively. The region out side the outer iris region with a radius of curvature marked as R4 about 7mm corresponds to sclera of the eye. This region is shown as 'D' in the fig.1.4. Marking of contact lenses done in the region specified as 'D' in the fig.1.4, as this region is not critical for the vision of the lens wearer [16].

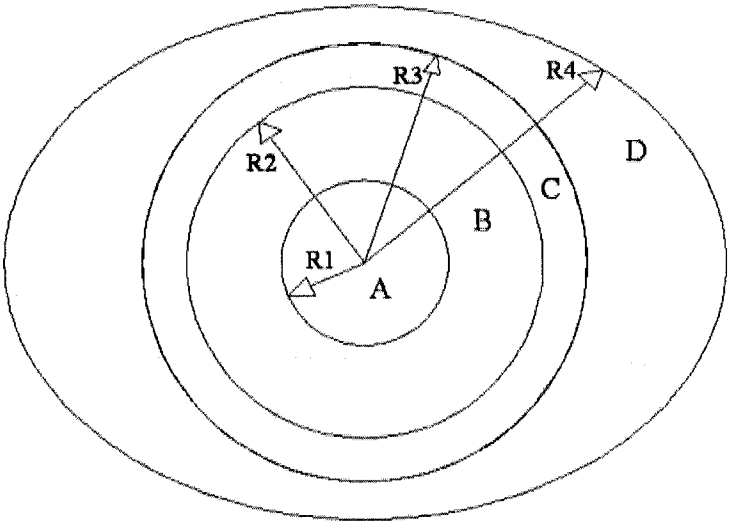

Fig.1.4 Different regions of lens corresponds to the respective eye position [16]

1.6.2 Dimensions for the marking

If marking is engraved on the contact eye lens, then dimensions of the marking depends mainly on two factors. First visibility of the orientation marks for the doctor, for fixing the orientation of toric lenses, second comfort of the wearer. Visibility of the mark can be improved by many ways as proposed in some literature.

(a) Visibility of the orientation mark can be improved if marking on the lens consists of a pattern of region of varying depth with in the boundaries of the mark. The method disclosed in the literature [17].

(b) The depressed region of the marking done on the contact eye lens reflects and focused light, therefore shape of the depressed region of the marking is critical for the visibility of the marks. Concave surface reflects and focuses incident light in such a manner that marking becomes more visible and prominent when viewed with slit lamps [18].

(c) Marking can also be done with one or more holes within the identifying mark instead of single line for improved visibility and comfort. The top of the holes of the identifying mark can be any shape i.e. square, rectangular, diamond and oval. The surface at the bottom of the holes has a common surface. Depth and ratio of width/depth as recommended for the holes for the identifying marks is in between 8-12 μm and 1.3 -1.6 respectively as plotted in fig.1.5 [18, 19].

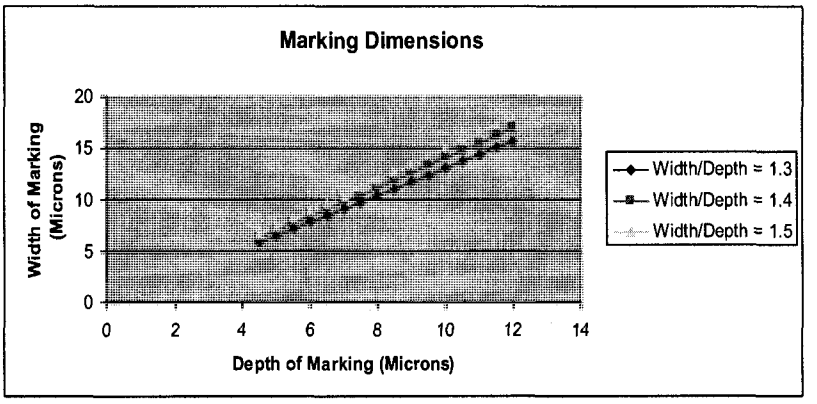

Fig.1.5 Width vs. Depth of marking

1.6.3 Marking Methods of contact eye lenses

Contact eye lens marking methods can be broadly divided in laser and non laser based marking respectively. Non laser marking methods are mostly chemical based methods. In one of the marking method, permeating solution was used for the marking purpose.

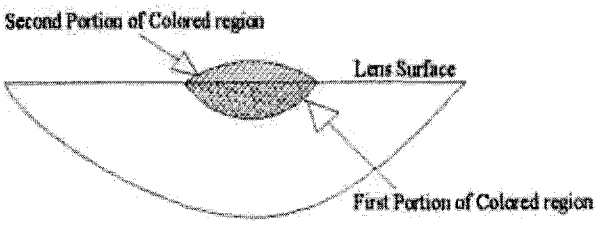

Fig1.6. Different zones of the color used for the marking on the lens surface [20]

In this method permeable solution to contact lens material is prepared by mixing pigments in organic solvent. This permeating solution is applied in association with

predetermined pattern masks on the contact eye lenses, which forms the colored regions as shown in fig.1.6. Second region formed on the surface of the lens is unwanted portion and so will be removed [20]. One more marking method described in the literature [21] also depends on the chemical based marking. In this marking method chemical are attached on the mold at a predetermined position in a specific manner such that when contact lens material will come in direct contact it will be polymerized with the lens material and forms a mark at a focused location on the lens.

Beside these chemical based methods there is some method which depends on mechanical methods of marking. Such methods involve Electro Discharge Machining [5].

1.6.4 Marking with laser

After discussing non laser based marking methods we are now moving into laser based marking of contact eye lenses. In one of the laser based marking method high energy laser pulses in the range of (1-3J/cm2) at a wavelength of 10.6 micrometer and pulse width of one micro second was used for direct marking of the contact eye lens [22]. As the pulse energy and pulse width used in the proposed marking method is very high so conduction of heat in the lens will be more, which deteriorate the quality of the marking as well as affects the quality and functionality of contact eye lens.

1.6.5 Marking with ultra fast laser inside the lens

In this most recently proposed marking method, femtosecond laser was used to create marking inside the contact lens. As femtosecond lasers have well defined threshold fluence therefore femtosecond pulses were used to create whitened portion inside the contact lens at half the thickness. One of the advantages of this type of marking is no protrusion on the lens due to marking. But femtosecond lasers are not very common for industrial application due to its high cost and downtime. Also direct contact marking methods are time consuming so not suitable for high throughput manufacturing [23].

1.6.6 Marking of metal mold inserts with laser beam

In another laser based marking method described in literature [6], masks with laser beam steering system was used for the marking of metal mold inserts. Marks created on the metal inserts were then subsequently transferred on contact eye lenses by injection molding. Mask used for the marking purpose is shown in fig.1.7. Advantage of this marking method lies in the method of marking. Instead of single big diameter spot, three small spots were used to cover the marking width which is evident from the profile of the mask as shown in fig 1.7. Contact eye lens with the discussed marking is shown in fig.1.8. But this marking method is little bit cumbersome due to mask designing and beam steering mechanism involved.

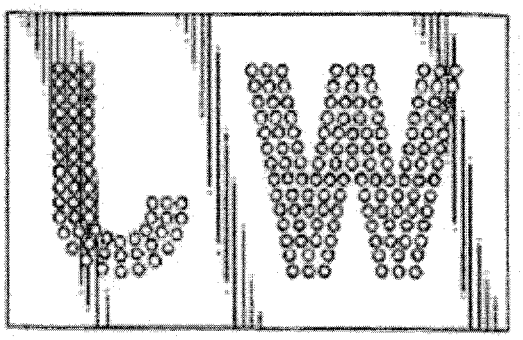

Fig1.7.Mask for the laser marking [6]

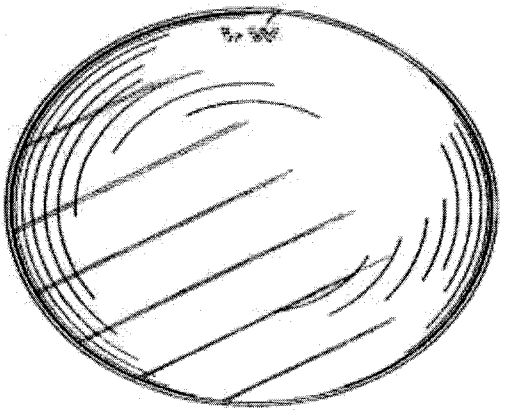

Fig.1.8 Marking done at the outer periphery of the contact lens [6]

1.7 Introduction to Lasers

Laser mechanism is shown in fig.1.9 [25, 26]. Laser basically converts electrical energy into high intensity light beam with stimulation and amplification [24]. Stimulation is a process in which electrons of the lasing medium (which can be gas, liquid or solid) are excited by an external source.

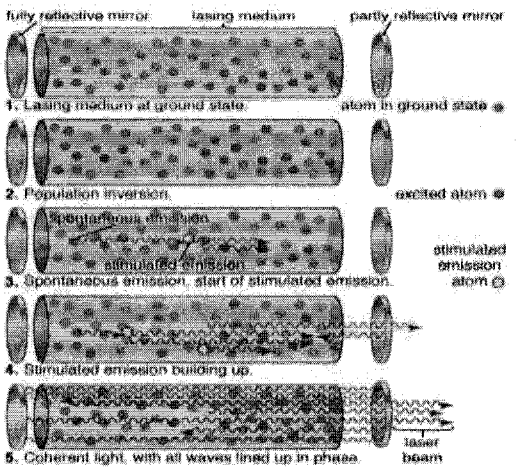

Fig.1.9. Schematic view of laser mechanism [24]

In the laser generation initially electrons of the lasing medium gains energy and are excited to higher unstable energy states. When these electrons transits from higher energy states (unstable) to lower energy (stable) state then laser light (photons) is created and wavelength of the laser light is a characteristic of the lasing medium used.

1.7.1 Laser Properties

Laser light emitted from the optical resonator will be highly monochromatic. High monochromaticity means short spatial bandwidth in terms of wavelength [27]. One of the advantages associated with laser light is its low or very limited diffraction or in other words laser light is a highly collimated light beam. Due to its low divergence laser light is transmitted over a small solid angle. Thus, laser light source possess extremely high radiance [26]. Another important property of laser light is its spatial and temporal coherence. The coherence refers to the connection between the phase of light waves at

one point and time, and the phase of the light wave at another point and time. Laser light is considered highly coherent in nature when compared with other light sources.

1.7.2 Laser types

Lasing medium is the most important part of the laser system. Laser can be classified on the basis of laser medium. Lasing medium can be either gas, liquid or solid [28-31].Further more all laser types operate in one of the two temporal modes continuous wave (CW) mode and pulse mode. In continuous wave mode the laser beam is emitted without interruption, whereas in pulse mode, the laser beam is emitted periodically.

Continuous wave (CW) operation of laser means that the laser beam is continuous in nature. Long pulse laser also comes in this category. In continuous laser, machining of material takes place by heating and then melting of the material. As heating and melting is the key phenomenon behind continuous laser machining, so this type of machining always results in recast layer and high heat affected zone [32, 33]. Due to low quality of machining, continuous lasers are not considered for most of the industrial and research purposes.

In pulse laser pulses with high energies and shorter pulse width can be produced by using any of these mechanisms as Q switching, mode locking, Cavity damping and gain switching [34].

1.8 Pulsed Laser Surface micromachining

Pulse laser micromachining is based on the interaction of laser light with the material. As highly focused short pulsed width pulses interacts with the matter so only small amount of material is removed in laser micromachining. Pulse laser based micromachining can be divided into two metal removal methods, pyrolithic (thermal) and photolithic processes [35-38]. Pyrolithic process is associated with Nano and micro second pulses. In pyrolithic process material is removed by rapid heating, melting and partial evaporation of the heated volume of the material. On the other hand photolithic process is the phenomenon of material removal associated with ultra fast laser pulses as pico and femtosecond lasers. In photolithic processes the photon energy is sufficient to break chemical bonds in material removal [38].

1.8.1 Femto second pulse micro patterning

Femto second lasers are mostly used for the research work related to surface patterning and sub micron machining. In femto second lasers the fluence of the laser beam can be tightly controlled in such a way that submicron feature size can be machined. It means that in femto second threshold is well defined. With femto second lasers the limitation of minimum feature size can be crossed [44-46]. Principle behind the material processing with femto second lasers is multi photon absorption, multi-photon absorption does not depend on the presence of free electrons therefore most of the materials can be processed with femto second lasers, even transparent materials like glass can also be processed with femto second lasers. The thermal diffusion time between two electrons is in the range of pico seconds, therefore no heat affected zone will be created

with femto second laser or no energy is transferred to the lattice. The ablation depth per pulse in femto second is given by

$$Z_a \approx \alpha^{-1} Ln\,[F_a/F_{th}] \qquad (1.1)$$

Where Z_a is the ablation depth, F_a is the absorbed fluence; F_{th} is the threshold fluence and α is the absorption depth. Many researchers have shown in their research work that sub micron or sub wavelength features that can be possible with femto second lasers [47-49].Despite all these advantages, femto second lasers are still not common in industries due to their high down time, low average power and high initial cost.

1.8.2 Pico second pulse micro patterning

The thermal diffusion time between two electrons is in pico second range; therefore heat transfer between electrons takes place while processing material with pico second lasers. Due to ultra short pulses heat affected zone is smaller when compared with other long or short pulses. In contradiction to femto second lasers where no liquid phase exists during material processing, pico second laser have liquid phase. The ablation depth per pulse in picosecond lasers is given by equation 1.1 [39].

1.8.3 Nano second pulse micro patterning

Nano second ablation heats the melts the processing material therefore heat affected zone is associated with nano second lasers. The ablation depth per pulse is,

$$Z_a \approx \sqrt{(at)}\, Ln\, [F_a/F_{th}] \qquad (1.2)$$

Where Z_a is the ablation depth, F_a is the absorbed fluence, F_{th} is the threshold fluence, and $(a.t)$ is the thermal diffusion depth. Nano second pulses are considered to be a long time scale. The specimen is heated, and then the main energy is lost due to net conduction into the bulk of the material [39].

Femto second and pico second lasers are mostly used for the research application in the field of sub micron machining [40-43].The ultra short-pulse laser technology is not yet mature compared to nanosecond lasers. Nanosecond laser technology is mature and is widely adopted in the industry for micromachining and marking applications.

1.9 Laser Processing Parameters

Laser based machining depends on many key parameters. Laser power is the most important parameter among all other parameters [50]. Lower power laser will not machine properly and higher values of laser power increases conduction of heat into the material which reduces the quality of the finished products. Laser power should be kept at optimum level. Search related to pulse laser micromachining with respect to quality of machining is published in research paper [51]. Bordatchev and Nikumb described the relationship of energy of pulse vs. crated diameter, depth and volume in pulsed laser micromachining [52].

Profile of the energy distribution within a laser beam indicates its quality. If laser beam is tightly focused in such a way that energy is concentrated within focused spot size than it is considered as a high quality beam. Ho and Ngoi [53] reported that a sub-spot size micro-machining technique utilizing the phenomenon of short pulsed laser interference.

The peak pulse power is the maximum available power of each pulse. In pulse laser micromachining, peak power have greater significance as it indicates the actual energy available for machining and can be compared with the threshold of the material.

The pulse duration is important from the conduction point of view. Shorter the pulse width lesser will be the heat conduction between electrons, preferably pulse width of pulse laser have to be in the range of ultra shot for minimum heat affected zone [39].

1.10 Interferometry

Laser machining can be controlled by either controlling the laser beam parameters e.g. laser power, repetition rate (rep.rate) or machining time. But the machining dimensions and the region of machining can not only be controlled by these parameters. For selective machining in the focused spot interference principle has been brought into the research. If two or more light waves of the same frequency overlapped at a point, the resultant effect depends on the phases of the waves as well as their amplitudes. The resultant wave at any point at any instant of time is governed by the principle of superposition. The combined effect at each point of the region of superposition is

obtained by adding algebraically the amplitudes of the individual waves. At certain points, the two waves may be in phase the amplitude of the resultant wave will then be equal to the sum of the individual wave amplitudes. Therefore, the interference produced at this point is known as constructive interference. A stationary bright band of light is observed at point of constructive interference.

At certain other points, the two waves may be in opposite phase. Thus, the amplitude of the resultant wave is zero. Therefore, the interference produce at these points is known as destructive interference. Thus, we see that are distribution of energy took place in the region of interference. The phenomenon of interference is discussed in detail with all the mathematical equations in the next chapter of theoretical modeling

1.10.1 Two Beam Interferometry

For creating interference an optical setup is required which can divide the single laser beam into two separate laser beams along separate paths in such a way that both of them can be interfered. Stationary interference fringes can be created if the phase difference between the two separate beams remains constant with time. Two methods commonly used for creating interference are wave front division and amplitude division [54].

1.10.2 Interference in micromachining

Most of the micromachining application of laser are to cut, drill and pattern material in microscopic level [55]. Some research work is also going on in the field of laser machining with the use of interference principle. Kawamura et al. introduced a two-beam holographic method to encode surface relief and sub-surface micro gratings [56, 57]. Similar concept was found in the setup proposed by Zhai et al. for the fabrication of gratings in bulk polymer medium [58]. Oi et al. also proposed a fabrication technique for fiber Bragg gratings by pulsed laser Interferometry [59, 60].

1.10.3 Common types of interferometers used for micromachining

(a) Mach-Zehnder Interferometer

Researchers proposed several types of interferometer for the machining of grating on the material surfaces [61, 62]. One of the interferometer is shown in fig.1.10 (a). Laser beam in the set described in the fig.1.10 (a) was first divided at non-polarizing beam splitter BS_1 into beam 1 and beam 2.beam 2 reflects from mirrors M_3 and M_4 and successively focused by focusing lens FL_1 on the sample surface. At the same time beam 1 is reflected from mirror M_1, M_2 and then with mirror M_4 and is finally focused by the focusing lens FL_1 on the sample surface. Compensation plate is used in the path of beam 1. As the two parallel beams were focused by FL_1 and interferes exactly at the same point to obtain an interference patterns on the top surface of the sample [63]. With this method, the fringe spacing, d can be varied selectively based on

$$d=\lambda/2\sin(\theta/2) \tag{1.3}$$

Where λ denotes the laser wavelength and θ denotes the angle between the two intersecting beams. From d it is noted that d is inversely proportional to θ. beside that, θ is a function of two parameters, namely the distance between the two parallel laser beams, D, and the focal length f of FL_1

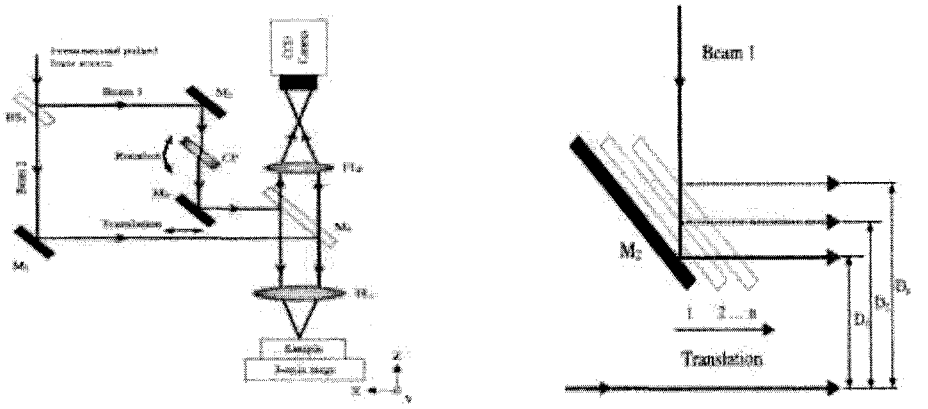

(a) *(b)*

Fig.1.10 (a) Adopted Mach-Zehnder Interferometer (b) Variation in pitch with M2 mirror [63]

Hence, in order to vary the fringe spacing, θ can be changed by varying either D or focusing lens. As such, M2 is introduced in the setup shown in fig.1.10 (a). To reflect beam 1 without obstructing beam2, M2 is translated to positions 1, 2, and n in order to obtain D_1,D_2 and D_n respectively as illustrated in fig.1.10 (b). Hence any d is attainable by translating M2 depending on the diameter of FL1.

(b) Interferometer for creating planar grating using common path configuration

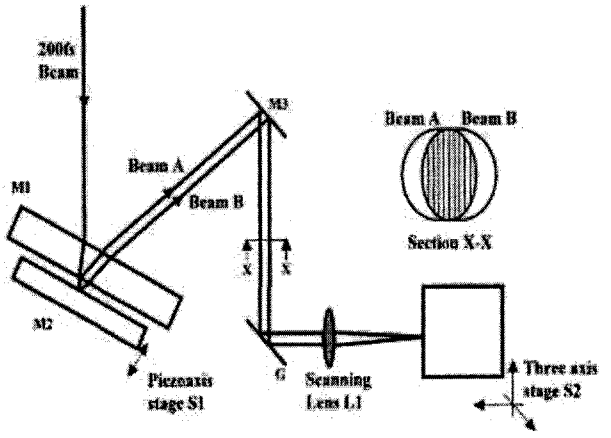

Fig.1.11 Interferometer machining setup [64]

The set up used for machining interference fringes is shown in fig.1.11. In the set up M_1 is the glass plate with special coating on the surface in such a manner that it reflects 50% of the incident light from the bottom surface as beam A and transmit the remaining 50%. One more mirror M_2 was kept in close proximity of M_1 for reflecting back transmitted 50% light as beam B. The two light beams A and B combine together at the focal length of lens L_1. The number f fringes machined on the sample surface can be controlled by varying the distance and angle of mirror M_2 with respect to mirror M_1 [64]. The number of fringes machined by this setup is limited by the distance between mirrors M_1 and M_2. No fringes will be formed if distance between the two mirrors exceeds coherence length of the laser used.

(c) A Three Mirror Interferometer for excimer laser

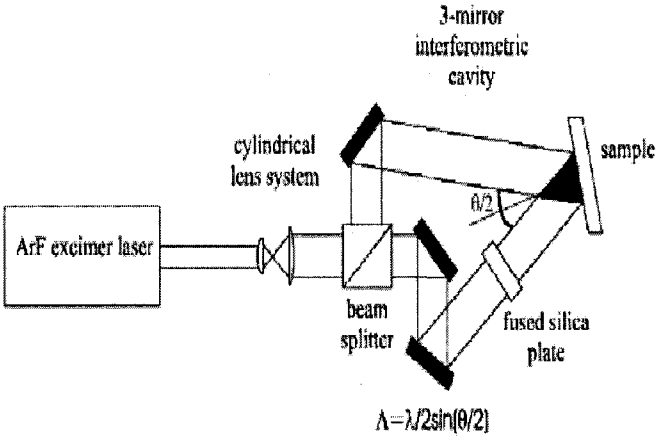

Fig.1.12 Three mirror interferometer [65]

A three-mirror interferometer was used to create a UV interference pattern on the surface, illustrated in fig.1.12. A two-lens cylindrical telescope was used to allow the beam area on the sample to be adjusted. The three-mirror approach was used to avoid wave front inversion at the sample, which is necessary since the excimer laser beam has low spatial coherence [65].

(d) Optical setup for creating fringes at the common focal point

This optical setup consists of three Wollaston prisms (W1, W2 & W3).The first Wollaston prism W1 as shown in fig.1.13 was used to divide the circularly polarized laser beam into two equal power beams. The divided beams coming out from W1 have opposite polarization, therefore half waveplate (WP) was used with one of the beam to

reverse the polarization and to make the polarization of the two beams same. Another wave late (WP) was also used with other beam to compensate the path difference. After this W3 and W4 were used to made the beams parallel and finally both the beams were focused with the common focusing lens (LE) as shown in fig.1.13

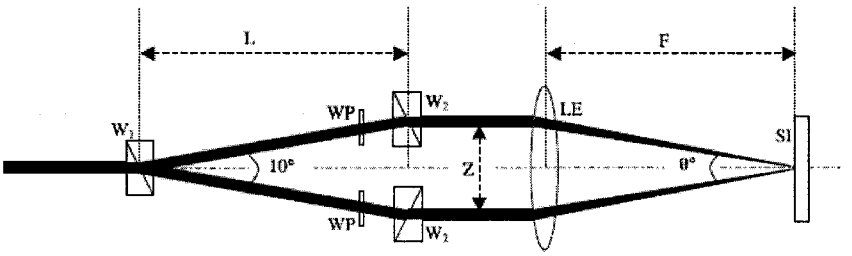

1.13 Optical setup [80]

1.11 Definition of the Problem

Marking of contact lens especially for the toric lenses is one of the critical steps in lens manufacturing. Proper marking not only helps the practitioner to fit the toric lens with proper orientation, but also improves the comfort of the wearer without interfering with his or her visibility. Dimensions of the orientation marking should be such that it is clearly visible at the time of setting, so that proper orientation of the lens with the cylindrical axis is assured. On the other hand dimensions must be small enough so that it will not create any discomfort or obstruction in the visibility of the wearer.

Commonly used marking methods for the marking of the contact lenses are EDM, Chemical method and Laser machining. In these methods either so much chemistry in

marking or it consists of complicated techniques such as mask designing and alignment of the mask laser marking. Whereas in EDM marking dimension are limited to the diameter of the rod.

1.12 Objective of the work

The objective of the research is to design a new marking method for toric contact eye lens. For better visibility of the marking with slit lamps the preferred ratio between depth and width of the marks is kept in between 1.3 to 1.5. In fig.1.5 different widths of marking are plotted against values of depth and from the fig 1.5 it can be calculated that required depth of marking lies in between 5-15 μm and width somewhere in between 12-18 μm.

To increase the visibility, the marking is preferably made up of two, three or more segments across the width of each marking. In the proposed interference principle based marking of the toric contact lens inserts; the number of fringe patterns across the width of marking as shown in fig 1.15 can be easily controlled with different focusing lens as showing fig.1.14. Our objective is to reduce the depth and width of the marking while increase number of patterns across the width of the marking as shown and compared with the old marking method in fig.1.14. The proposed marking method will reduce the marking area and will increase the comfort of the wearer without compromising the visibility of the marks.

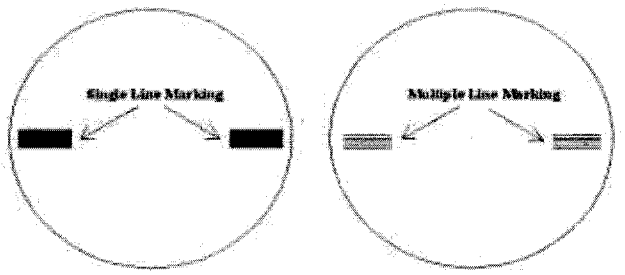

Fig 1.14 Proposed Toric Contact Lens Marking Methods

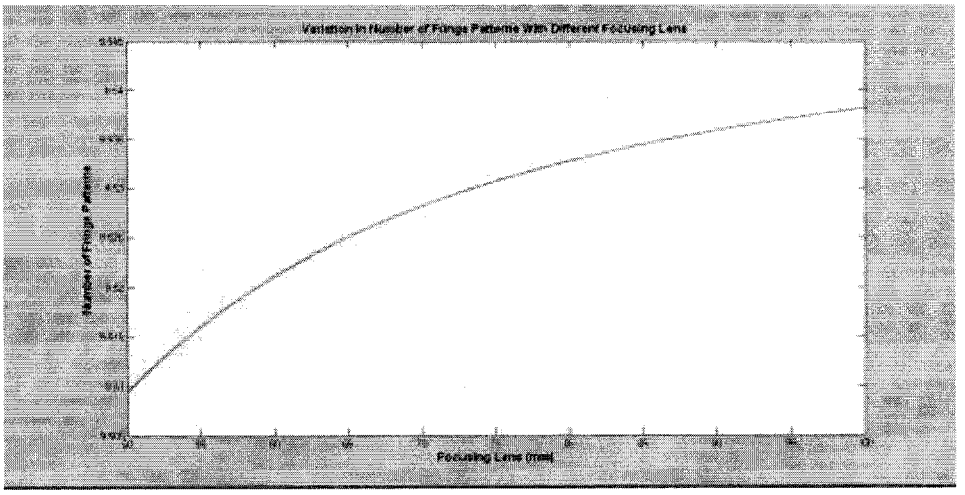

Fig.1.15 Number of lines machined within focused spot size

1.13 Scope of work

Proper theoretical modeling of the machining parameters and aspherical surface of the lens has been done, which can predict the optimum machining parameters of the laser for the designed marking of lens. Designing of marking dimensions for better visibility and comfort of the wearer. Designing and aligning the optical set up for the

proposed marking method. Experiments will be planned to study the affect of different laser parameters with respect to quantity and quality of the marking.

1.14 Summary

Trend of contact eye lenses are increasing day by day. Different type of contact lenses is available in the market, for specific purposes. Each and every contact lens bears some kind of marking on it which help in deciding the type of contact lens and also sometimes may be used for maintaining the inventory and quality in the production. Besides all these functions of the marking the most critical function of the marking is to help in aligning the toric contact eye lens with the cylindrical axis of the patient suffering from astigmatism.

Presently several marking methods have been registered as patents. As discussed in the literature review that there are some short comings in the existing marking methods, either the methods are time consuming or marking requires different set of masks for different marking dimensions. To address these issues a novel pulsed laser based marking method is proposed for toric lens inserts on the principle of interference along with a simple optical setup that can be easily tuned for different marking dimensions.

Chapter 2

Theoretical Modeling

2.1 Introduction

Theoretical modeling has been done to predict the behavior of laser marking on the Contact eye lens inserts. For predicting the marking behavior the whole modeling has been divided in two parts.

In the first part of the modeling the surface of the toric contact eye lens has been modeled and compared with the surface of eye cornea, thereafter the marking region has been located on the contact lens inserts according to the discussions done in section 1.8.1. As, the modeled surface of the toric contact eye lens is aspherical in nature, so variation in marking depth has been predicted within the machined spot with respect to intensity and depth of focus.

Second part of the modeling has been done to predict the machining or marking of stainless steel the mold insert material with respect to different laser parameters e.g. laser power, rep.rate and time of machining.

2.2 Asphericity of the male insert

Modeling has been started with simulating the aspherical surface of contact eye lens. Aspheric designing of rigid lens was initially described by Nissel in 1966 [66]. The cornea of human eye is not spherical and is considered as aspherical in shape which can be described by an ellipse having a numeric eccentricity (e value) of 0.45 [67, 68]. Various aspheric mathematical models to describe the complex shape of the anterior corneal surface have been proposed [69-75].The mathematical equation used for the modeling of the contact eye lens surface is

$$Sag_c = \{r_o - \sqrt{(r_o^2 - y^2 p)}\}/p \qquad (2.1)$$

Where y is the distance to corneal center at the point where sag is calculated, r_0 is the posterior apical radius of curvature. Apical radius is the radius of curvature for the inside of the contact lens, the surface that touches the cornea; p is the shape factor of the cornea and Q is the asphericity ($p = 1 + Q$) [75]. Recent studies found that human cornea Q-values vary significantly with age [76]. Effect of Q values on the cornea surface is show in fig.2.1 [76]. It can be seen in the fig.2.1 that with the increase in the asphericity the sag values are also increasing in the center; therefore it can be said at this point of modeling that asphericity is also an important factor needs to be considered while manufacturing or deciding the contact eye lens surface profile.

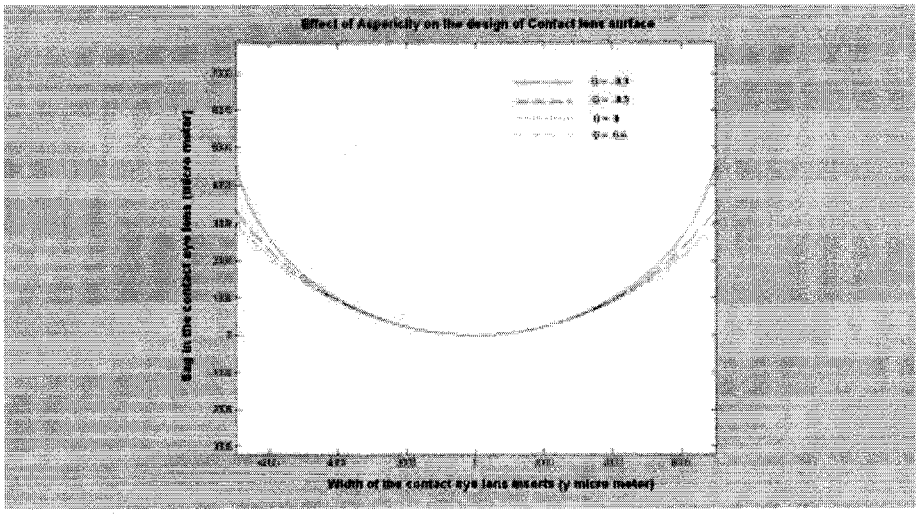

Fig.2.1 Affect of asphericity on contact lens surface [76]

For the modeling of the contact lens insert surface the value of asphericity (Q) selected has the standard value of -0.262 and the value of apical radius of curvature was selected as 7mm according to the research published in paper on changes in asphericity with age [75]. Surface of the contact eye lens metal inserts as shown in fig.2.2 has been modeled with the help of equation (2.1). As mentioned in the section 1.8.1 that region of marking lies in the periphery of the contact eye lens, therefore while modeling for the surface of the inserts the region of marking has been also modeled and shown in the fig.2.2 along with the contact lens inserts surface with a darker portion on the same profile of the surface. For better understanding of the region of marking on the contact lens insert laser beam is also plotted in fig.2.2 which is perpendicular to the marking surface.

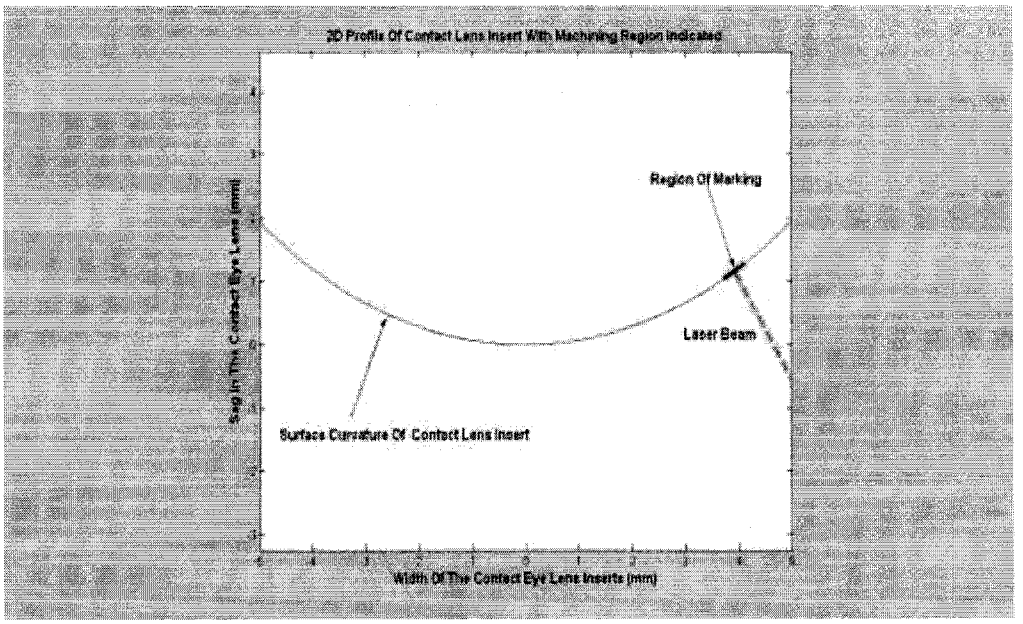

Fig.2.2 Marking Region on the modeled toric lens insert

2.2.1 3D profile of the Contact lens Surface

For the better understanding of the marking region on the insert a 3D profile of insert surface has been plotted in fig. 2.3 and the marking region has been shown with red color strips.

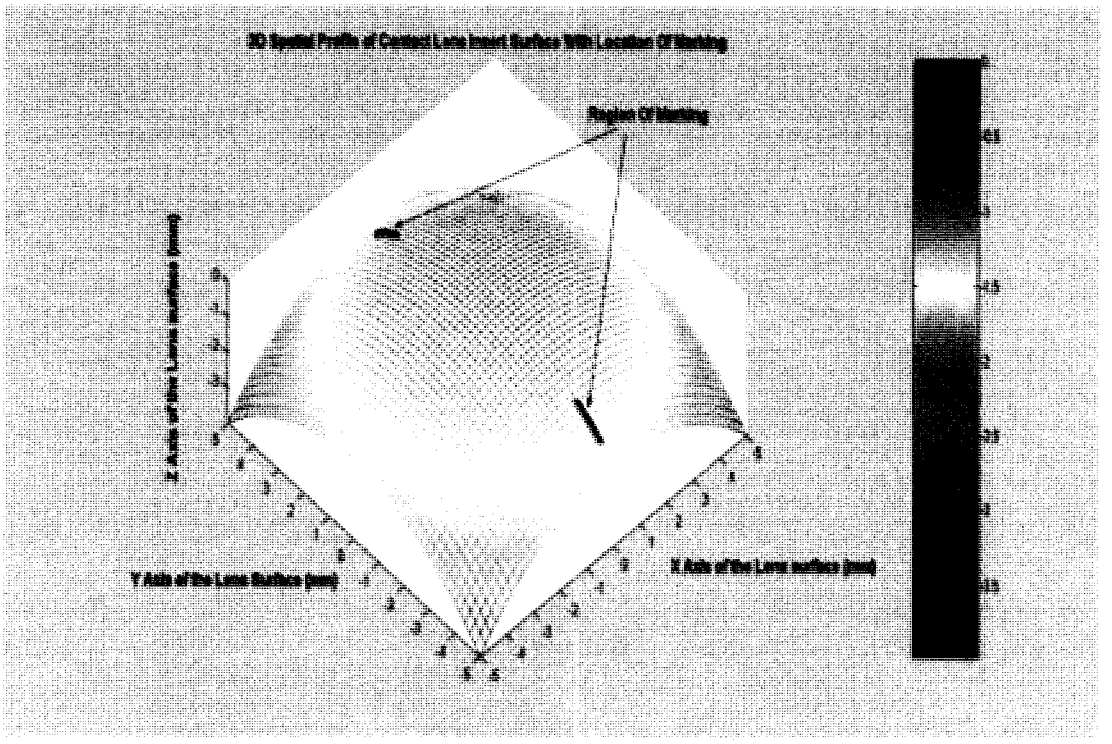

Fig.2.3 3D Profile of Contact Lens Insert

2.3 Effect of asphericity on marking depth

In the proposed marking method no steering mechanism was involved for the laser beam therefore there will be some variation in the depth of the marking within marked region or area due to the aspherical profile of the lens insert. Marking is proposed with cylindrical focusing lens so that laser beam will be focused along one axis and remain unfocused in the other plane of axis. Required length of the marking according to research dimension of the marking specified by Jongliang Wu et al [17, 18] is in between 0.7mm to 1.0 mm. For our research project calculation were done for marking length of 1.0mm (unfocused beam diameter) whereas the width of whole marking region was kept

at 200 μm the (focused part of the beam).The deviation of the curvature of the lens insert from the flatness was calculated along the length of the marking and is plotted in Fig.2.4

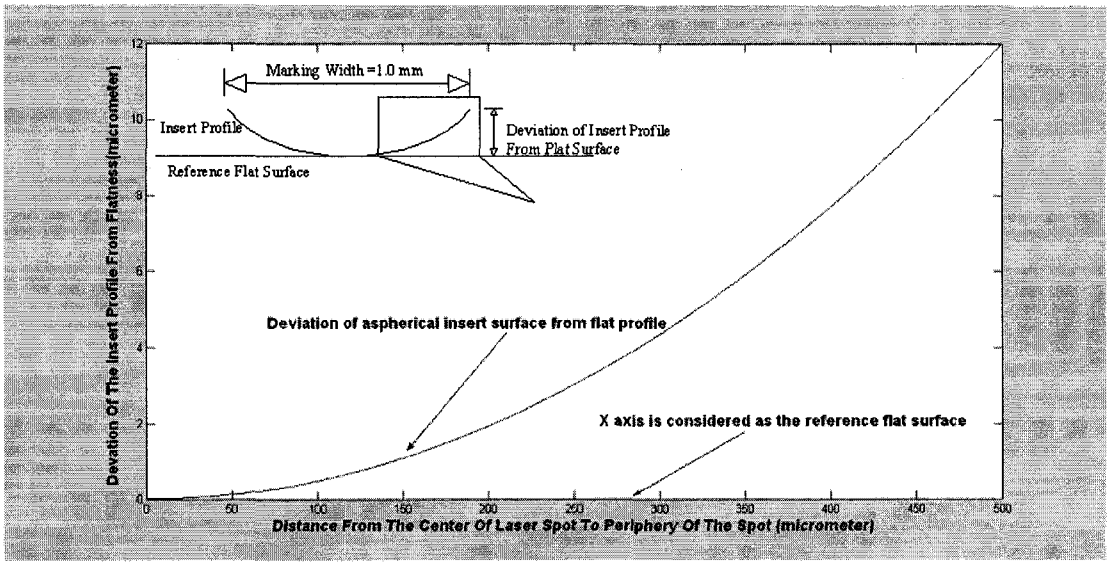

Fig.2.4 Deviation of Insert lens curvature with respect to flat surface along the length of the marking

From the Fig.2.4 it can be seen that the deviation in the insert curvature with respect to flat surface is approximately 12μm along the length of the marking. From the above description of Fig.2.4 it can be concluded that for marking whole length of 1.0mm the minimum depth of marking must be kept above 12 μm so that none of the region along the length will be left unmarked.

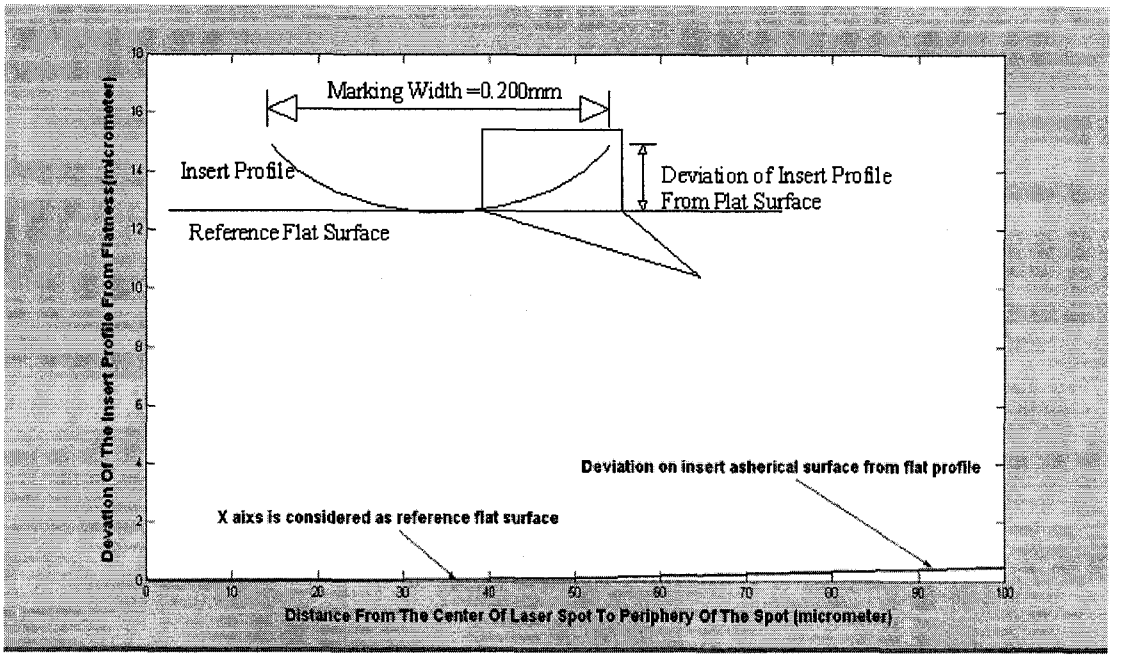

Fig.2.5 Deviation of Insert lens curvature with respect to flat surface along the width of the marking

Fig.2.5 Shows the deviation in the curvature of the lens inserts along the width of the mark (focused part of the laser beam). It can be seen from the fig.2.5 that the deviation along the width of the marking is less then 0.5μm or can be considered negligible when compared with the deviation along the length of the mark

2.4 Intensity distribution with or without interference

Theoretical model has been prepared for comparing the intensity distribution at the focusing spot with or without interference of laser beam. Gaussian beam profile is considered for all the modeling part. Laser beam can be tuned for different beam

diameters with the use of beam expander, but for the modeling part only one beam diameter of 4.8mm has been considered.

Intensity distribution without interference is given by equation (2.3) and with interference is mentioned in equation (2.4) [78]

$$I=I_1+I_2 \tag{2.3}$$

$$I=I_1+I_2+2\sqrt{(I_1I_2)}\,Cos\delta \tag{2.4}$$

Where

I = Intensity Distribution within focused region

I_1 and I_2 = Intensities of two separate laser beams respectively

δ = Phase difference between the two beams

$2\sqrt{(I_1I_2)}\,Cos\delta$ = Interference term

From the equation (2.3) it can be seen that when two beams with intensities I_1 and I_2 meet and have interference then the total intensity is not only the sum of the intensities, but the term $2\sqrt{(I_1I_2)}\,Cos\delta$, known as the interference term will appear in the final intensity. The intensity of the interfered beam depends on the phase difference which can be varied from 0° to 180°. Whenever the two interfering beams have zero phase difference the total intensity become I_{max}.

$$I_{max} = I_1+I_2+2\sqrt{(I_1I_2)} \tag{2.5}$$

When $I_1 = I_2 = I_0$

$$I_{max}=4I_0 \tag{2.6}$$

But when the phase difference δ is 180 then in that case the sum of intensities will become

$$I_{min} = I_1+I_2 - 2\sqrt{(I_1I_2)} \tag{2.7}$$

If $I_1 = I_2 = I_0$

Then $$I_{min} = 0 \tag{2.8}$$

For the better understating of intensity distribution with or without interference, intensity distribution has been plotted within focused spot, if a laser beam of 17.85kW peak pulse power, rep rate of 20 kHz is focused with a focusing lens of 100mm.

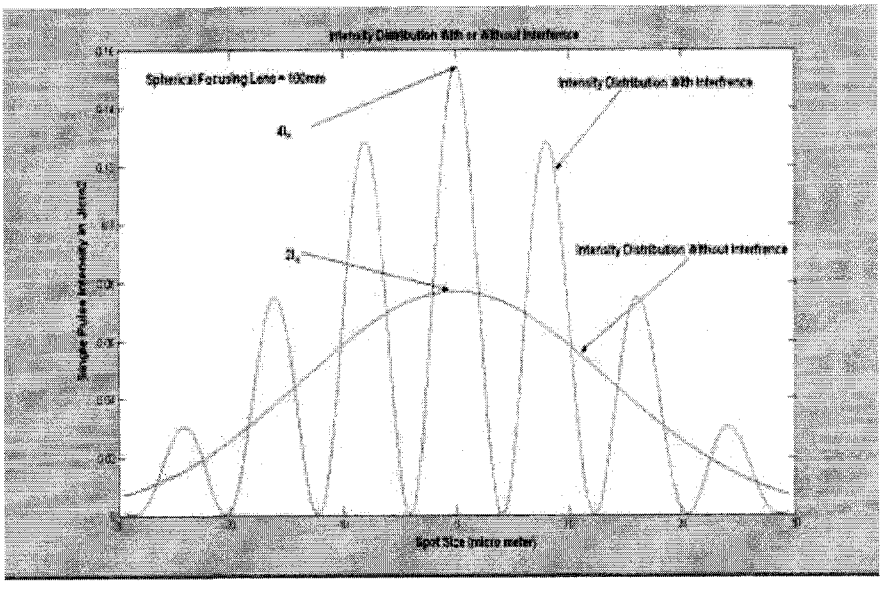

Fig.2.6 Intensity distribution curve

From the fig.2.6 it can be seen that with interference the intensity distribution at the constructive points will be increased up to 2 times more then the intensity distribution at the same point without interference. From the modeling of intensity distribution with or without interference it can be predicted that the heat affected zone of the machining region can be reduced by using interference concept. Due to interference 1/2 of the power is required for machining the same depth as machined without interference.

2.5 Machining with different laser power

As discussed in the previous section that Gaussian beam profile has been considered for the theoretical modeling. From machining point of view the machining spot size will depend on the laser power and type of laser used. Radial distance up to which the beam intensity will decrease to 50% (Full Width Half Maximum) of the maximum is considered as the spot radius if the ultra shot laser is used. But in nanosecond laser when the ablation threshold is not well defined like the femto second laser then 86.4% of maximum ($1/e^2$) will be considered as the spot size.

In fig.2.7 machined spot size with respect to power of 1 watt has been shown. Based on the threshold of the stainless steel (lens insert material) the ablation starts at 0.16J/cm2. As seven fringes have intensity above threshold ablation value of stainless steel so only these seven fringes will take part in machining and rest four fringes will not take part in machining. From this analysis it can be predicted that while machining with 1 watt laser power seven fringes can be machined

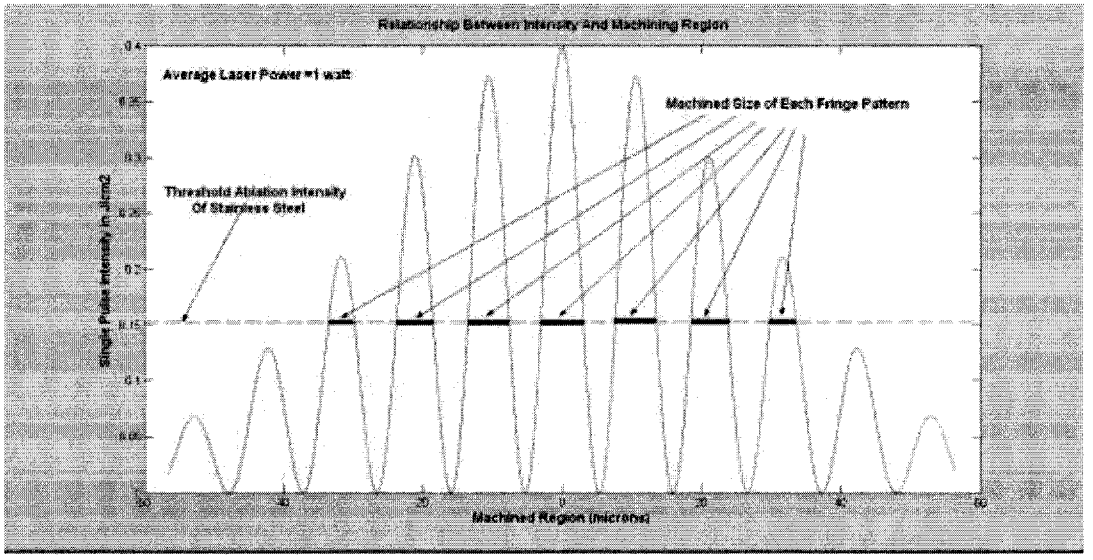

Fig.2.7 Machined size of fringe patterns with 1 watt of peak pulse power

Now for the next part of the modeling intensity distribution of laser pulse has been plotted in fig.2.8 with an average laser power of 2 watt. As mentioned above that 0.16J/cm2 is the minimum fluence required to start the machining of stainless steel.

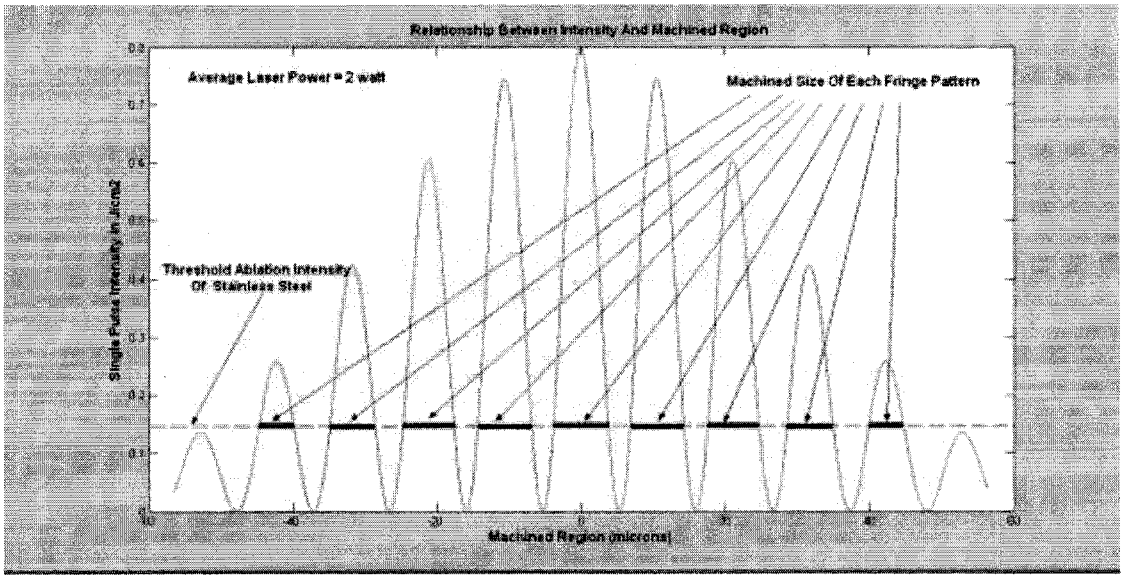

Fig.2.8 Machined size of fringe patterns with 2 watt of peak pulse power

From fig.2.8 it can predicted that if machining will be done at 2 watt then instead of seven, nine fringes will be machined, as nine fringe patterns have the fluence above 0.16J/cm2 (ablation threshold of stainless steel). From this part of the modeling it can be concluded that with increase in power the machining region will be increased also the size of the fringe patterns machined in the center of the region will increase as can be predicted from comparing the pattern size in fig.2.7 and fig.2.8.

2.6 Depth of Machining with laser power

Modeling has been done for predicting the variation in depth with corresponding variation in laser beam intensity. As the laser system for which modeling has been done is an Nd: YVO4 laser with a pulse width of 14ns, therefore ablation took place either by thermal diffusion or by the melting of the material to be ablated. Mathematically depth of machining with nanosecond lasers can be calculated with equation (2.9) [39]:

$$L=\sqrt{(a.t)}\ln(I_a/I_{th}) \tag{2.9}$$

a= thermal diffusivity (μ^2/sec)

t = pulse width of the laser (14 nano second)

I_a=absorbed fluence (Absorbed fluence on the surface of material at particular wavelength.)

I_{th}=threshold fluence (Threshold fluence for stainless steel is 0.16J/cm^2) [79]

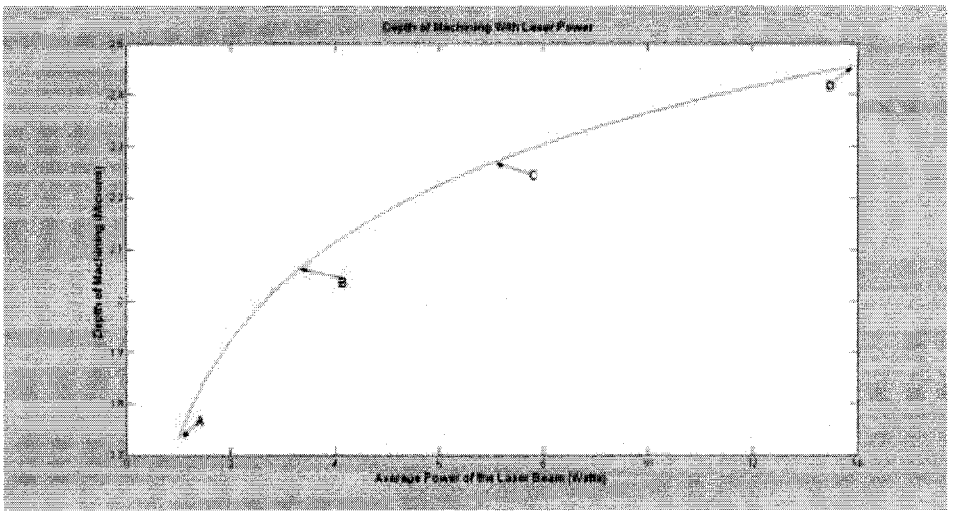

Figure2.9 Depth of machining with different laser pulse power

In fig.2.9 depth of each machining with respect to different power has been plotted. Stainless steel depth of machining is simulated with an absorption percentage of 40% for the wavelength of 1064nm. The plotted curve has been divided in three zones according to the slope of the curve. Region one is starting from A to B it corresponds to machining depth at a power of 1 to 3.7 watts. In this region the slope of the curve is steep. Second region is in between B and C which corresponds to laser power ranging from 3.7 watts to 7.2 watts. In second region slope of the curve is not as steep as it was in region one. Third region is in between points C and D and this corresponds to high laser power. In the third region increase in the depth is not as significant as in first region. Most of the energy supplied in the thirst region will decapitated in the stainless steel without indenting too much depth. From the three regions shown in the fig. it can be predicted that the region two is best for the machining with less heat decapitations. With the increase in machining time the number of pulses hitting the surface will increase which

ultimately increases the depth of machining. The depth of machining shown in the fig.2.9 is for the single pulse. More the pulses hit the surface more will be the depth of machining achieved.

2.7 Depth of machining with repetition rate

Depth of machining has been predicted with the change in the rep. rate of the pulsed laser. In the pulsed laser, ablation of material depends on the peak power of each laser pulse. With the increase in the rep rate number of pulses hitting the surface will increase with an increase in average pulse power.

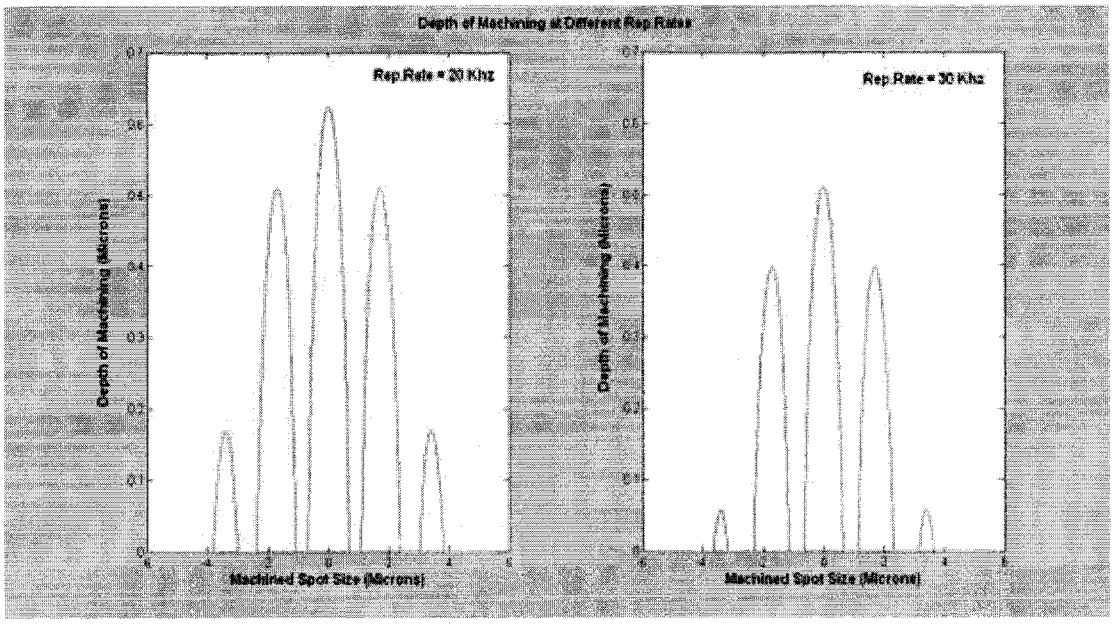

Fig.2.10 Depth of machining with different rep rates

From the subplots of fig.2.10 it can be predicted that with the increase in rep rate depth of machining will be reduced. The relation between the energy of each pulse and rep rate is given by the equation 2.10:

$$E=P/R \tag{2.10}$$

Where

E= Pulse energy in Joules

Pulse width = 14ns

P=Average Pulse Power in watts

R= Rep.rate in Hz

P_{peak} = Peak Power of each laser Pulse

$$P_{peak}=E/pulse\ width \tag{2.11}$$

Peak power of the pulse laser can be calculated using the equations (2.10) and (2.11) respectively. Pulse average power of the laser beam at 30 kHz of rep. rate and 34 amperes of diode current is 14watt according to the specification given by the laser manufacturer. By using equation (2.10) and (2.11) peak power of each pulse can be calculated as:

$$E = 14/30*1000 = 4.67*10^{-4}$$

$$P_{peak} = 4.67*10^{-4} / 14*10^{-9}$$

$$P_{peak} = 33kW$$

Peak power obtained at 30 kHz of rep rate is now compared with the peak power of the pulse at 50 kHz of rep rate and at a value of 34 amperes of diode current with an average laser power of 16.5 watts.

$$E = 16.5/50*1000$$

$$P_{peak} = 3.3*10^{-4} / 14*10^{-9}$$

$$P_{peak} = 23.5kW$$

Now from the above equation (2.10) and the subplots it can be predicted that with increase in the rep rate energy of each pulse will be decreased, which ultimately reduces the machined depth.

2.8 Variation of pitch of patterns

Theoretical modeling has been done for predicting the variation in the pitch according to the earlier research done [63]:

$$d = \lambda/2 \sin(\theta/2) \qquad (2.12)$$

In equation (2.12) d is the pitch of the fringes, θ is the angle between the two focusing beams and is the wavelength of the laser beam. From the equation (2.12) it can be predicted that pitch of the fringes can be changed by varying the angle between the two focusing beams.

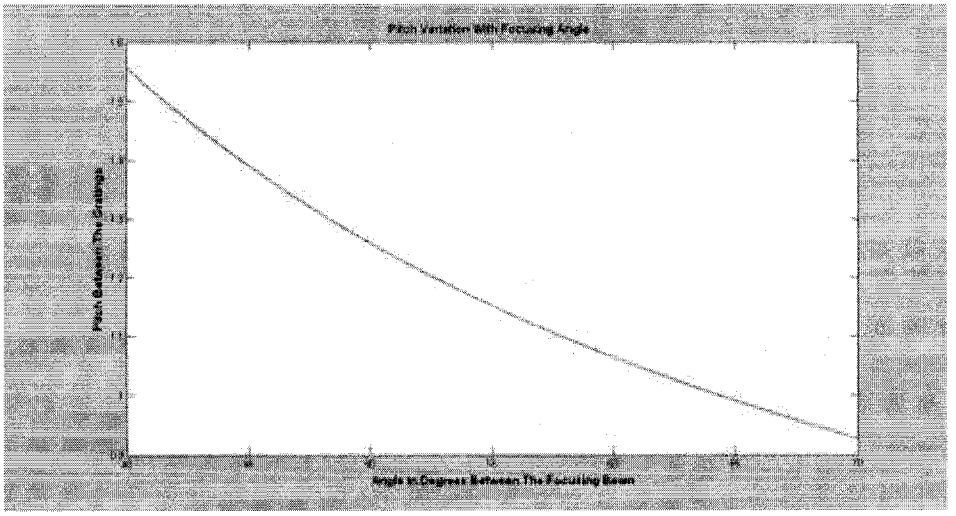

Fig.2.11 Pitch variation with focusing lens and beam spacing

From the fig.2.11 it can be predicted that by decreasing the angle between the focusing beams pitch of the fringes can be increased and vice versa by increasing the angle between the focusing beams.

2.9 Summary

From the theoretical modeling it can be summarized that the surface of contact eye lens inserts are aspherical in nature. Different laser parameters have been studied and affect of those parameters on machining has been predicted. From the results of the modeling it can be concluded that area of machining can be controlled with the help of laser power whereas depth of marking can be controlled with all the three laser parameters laser power, rep.rate and machining time. One of the advantages of the proposed marking method is the experimental setup. Alignment of the setup is easy with the readily available optics and can be used in Industries as well for the production manufacturing.

Chapter 3

Experimental Setup

3.1 Introduction

As discussed in the objective of the research project, patterns need to be machined on the surface of the metal mold inserts which can be later transferred on the outer surface of the toric lens through the molding process. For creating these patterns on the metal mold inserts the machining setup selected for the machining was the one which can create interference at the focal point or the surface of the machining sample. Researchers have proposed many setups for marking by using the power of interfered laser beams for creating gratings or fringes on the flat surface as discussed in the section 1.13.3.In most of the commonly used setups for creating the fringes at the focus, laser beam alignment was the cumbersome task therefore, the setup selected for the experiments have several advantages as only single lens is required to focus both beams and pitch between the fringes can be easily varied with minimum change in the setup.

3.2 Explanation of the setup

The setup was designed and modified with the ability to form fringes at the focal point as discussed in the literature review. A pulsed laser beam from Nd: YAG laser is spatially filtered and the diameter of the beam is expanded to 4.8mm from 0.8mm diameter. The beam coming out from the laser is made circularly polarized using a quarter waveplate. The circularly polarized laser beam is made to pass through a 20^{o} first

Wollaston prism. The output of the first Wollaston prism is therefore two orthogonally polarized beams with an angle of 20° between them. In order to make these two beams parallel so that it can be focused at a common point using single lens, each of the two orthogonally polarized beams is made to pass again through two separate 20° Wollaston prisms as shown in the fig.3.1. It is important to note that, in order to get interference from the two beams, the polarization of one of the beams needs to be changed while maintaining the polarization of the other. Changing the polarization can be done by using a half waveplate on any one of the axis of the two beams.

Now the output beams from the Wollaston prisms 2 and 3 are collimated, parallel and are in the same polarization state. As the distance between the two parallel beams coming out of the wollaston 2and 3 are 30mm distance apart and most of the common optics have the diameter of 25mm so the two parallel laser beams were converged using the 500mm diameter length and then made parallel again by using the diverging lens of diameter 200mm to reduce the parallel beam separation from 30mm to 13mm which in turn reduces the beam diameter from 4.8mm to 2.3mm.

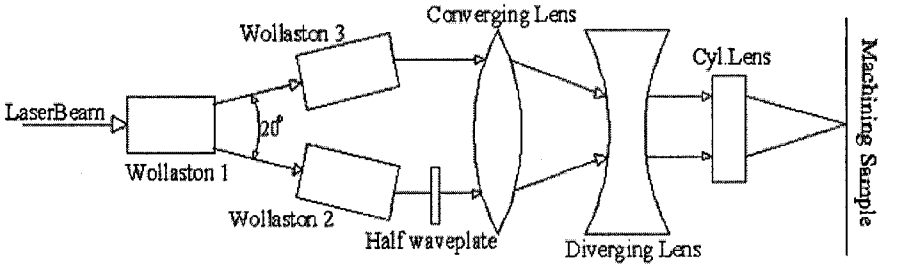

Fig3.1 Machining Setup with Wollaston prisms as the central element [80]

3.3 Details of laser optics used in experimental set up

The experimental setup selected and modified for the experiments have polarization optics as the main components. This polarization optics includes Wollaston prisms, quarter waveplate and half waveplate. Besides this polarization optics some focusing optics was also used to adjust the beam spacing. Now each and every component used in the complete experimental setup is explained in detail.

3.3.1 Nd: YVO4 Laser (Neodymium Doped Yttrium Orthvanadate (Nd: YVO4) Crystal)

Laser used for the experimental work was manufactured by Coherent laser. It is basically an Nd: YVO4 (Neodymium Doped Yttrium Orthvanadate) laser with an average continuous power of 14 watt. Laser belongs to the series of PRISMA 1064-16V. Laser medium was Nd: YVO4 with sealed long life pump diodes as the pumping source and acoustic optical Q switch as the pulsing unit.

Among the various existing laser crystals e.g. Nd: YAG, Nd: YVO4, Nd: YLF for solid state lasers, NdYVO4 is the most efficient laser crystal. The properties which make Nd: YVO4 crystal efficient among the other existing crystals are high absorption coefficient, high induced damaged threshold and good physical and mechanical properties [81].

Laser system can be tuned for different rep. rate. Rep. rate is the number of pulses coming out of the laser head in one second time. Laser can be tuned for rep rate values starting from 20 kHz to 100 kHz. One more parameter that can be varied for the

laser system is diode current, which can be increased from 13 to 34 amperes at all the available rep rates. With the increase in diode current average power will also increase. Peak power of the laser which is discussed in chapter 1 &2 is 30 kW at a diode current of 34 amperes and rep rate of 30 kHz.

3.3.2 Wave Plate

A wave plate is an optical device that alters the polarization state of a light wave traveling through it by principle of birefringence.

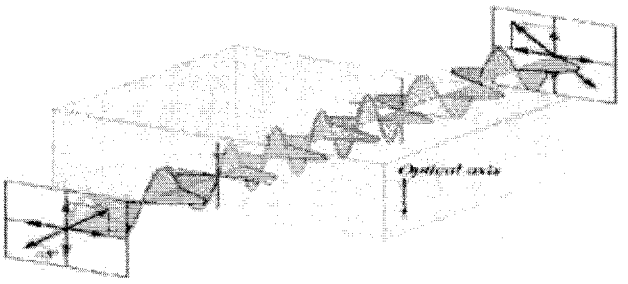

Fig.3.2 Waveplate [82]

Waveplates are a class of optical elements that serve to change the sate of polarization of an incident wave. The operation of a waveplate is very simple. When plane polarized light is incident on a waveplate, it splits the light into two plane polarized light waves and one of the wave's lags behind the other by a known amount. Upon emerging from the waveplate, the two waves superimpose on each other to produce a wave, which is of a different state of polarization. Quarter waveplate and half waveplate are two important Waveplates.

For instance a quarter-wave plate creates a quarter wavelength phase shift and can change linearly polarized light to circular and vice versa as shown in fig.3.2 and fig.3.3. Quarter waveplate is a thin plate of birefrigent crystal having the optic axis parallel to its refracting faces and its thickness adjusted such that it introduces a quarter wave ($\lambda/4$) path difference (or a phase of 90°) between the extraordinary-ray and ordinary-ray propagating through it.

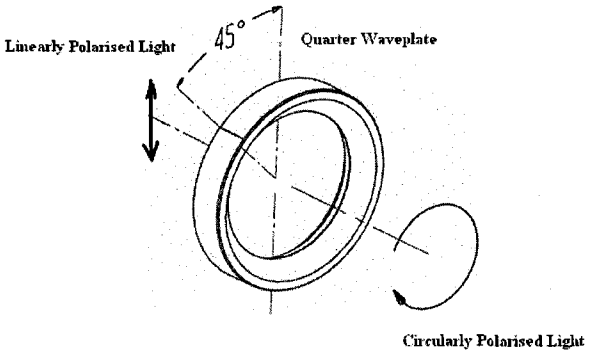

Fig 3.3 Working principle of Quarter waveplate [83]

When a plane polarized light wave is incident on a birefrigent crystal having the optic axis parallel to its refracting face, the wave splits into extraordinary wave and ordinary wave the two waves travel along the same direction but with different velocities. As a result, when they emerge from the rear face of the crystal, an optical path difference would be developed between them. Thus, for quartz waveplate path difference can be written as, [82].

$$(\mu_e - \mu_o)d = \lambda/4 \tag{3.1}$$

Where

d = thickness of the waveplate

μ_e = refractive index of waveplate for extraordinary light wave

μ_o = refractive index of waveplate for ordinary light wave

A half wave plate is a thin plate of birefringent crystal having the optic axis parallel to its refracting face sand its thickness chosen such that it introduces a half wave ($\lambda/2$) path difference (a phase difference of 180°) between extraordinary ray and ordinary ray. Principle of half waveplate is shown in the fig.3.4 the phase difference created by the half waveplate is shown as 180° (-90° to +90°).

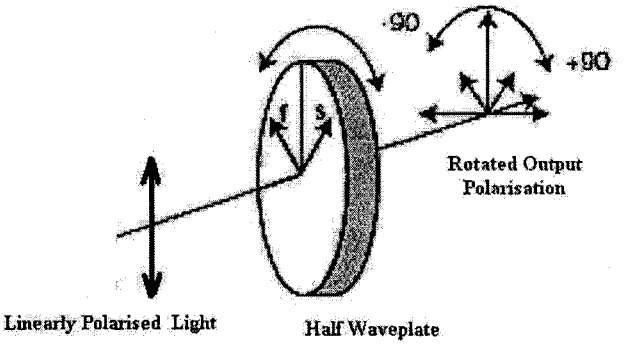

Fig 3.4 Working Principle of Half Waveplate [84]

The only difference between the half and the quarter waveplate is the thickness of the waveplate according to the desired path difference. Equation of path difference created by half waveplate is given as

$$(\mu_e - \mu_o)d = \lambda/2 \tag{3.2}$$

3.3.3 Wollaston Prism

Wollaston prism comes under the category of polarizing optics and is named after its name of the inventor 'William Hydne Wollaston'. Wollaston prism is basically two right angle calcite prisms cemented together with perpendicular optic axis.

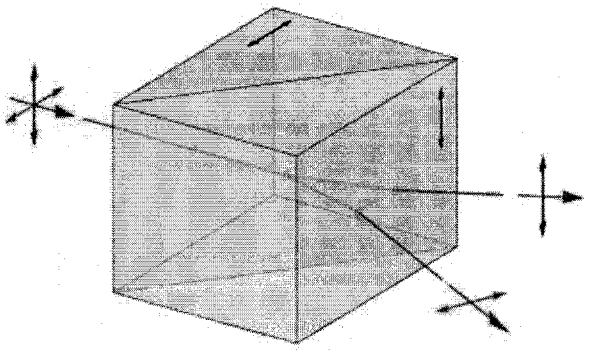

Fig.3.5 Wollaston Prism [85]

When a circularly or randomly polarized light enters in a Wollaston prism then two separate linearly but orthogonally polarized laser beams come as an output as shown in fig 3.5 [85].

3.3.4 Cylindrical Plano Convex Lens

Cylindrical lenses focus or expand light in one axis only as shown in fig.3.6.Since the patterning requirement of this project is long and thin lines therefore cylindrical lenses are used to focus the laser beams.

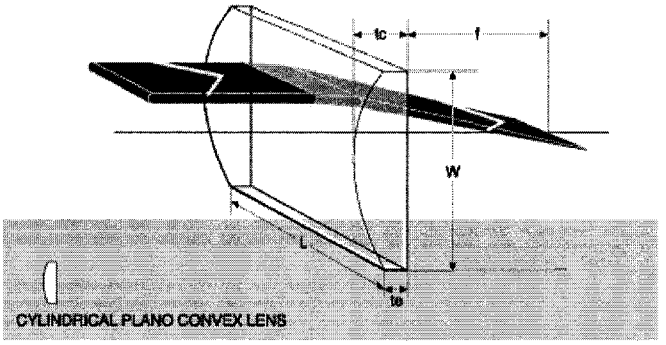

Fig.3.6 Cylindrical Lens [85]

Where

f = focal length of the cylindrical lens

t_c = Center thickness of Cylindrical lens

t_e = edge thickness of cylindrical lens

W = width of the lens

L = length of the lens

3.4 Optical Setup description

Alignment of the optical machining setup was done with respect to two parameters.

(a) Laser beam alignment with the horizontal and vertical axis.

(b) Laser power alignment for reducing the reflection and alignment loses associated with the optics.

3.4.1 Laser Beam Alignment

Two 45° reflection mirrors were used for steering the beam in vertical and horizontal axis. Laser head is heavy and it is almost impossible to align the laser beam with both the above mentioned axis. By using two reflecting mirrors as shown in fig.3.7 laser beam can be easily aligned with the help of leveling screws of the mirror holders the laser beam was first aligned with the vertical axis and then with the horizontal axis with respect to the vibration isolation table surface.

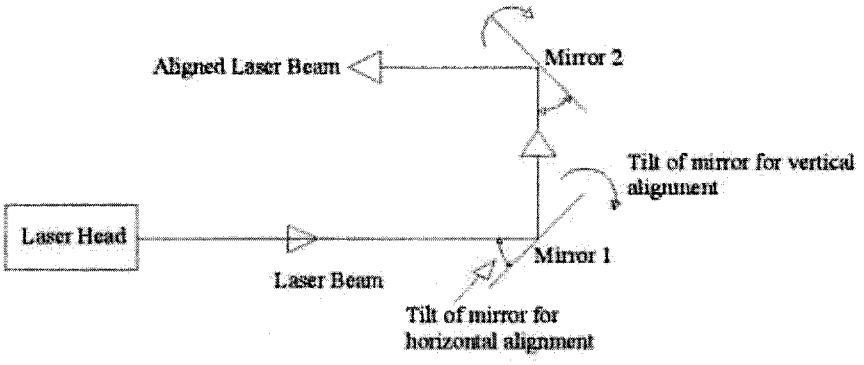

Fig 3.7 Laser beam alignment

3.4.2 Alignment of first Wollaston prism

After aligning the laser beam with the horizontal and vertical axis the next important task was to align the laser optics for maximum transmissive power efficiency from each of them.

Transmissive Efficiency = Power Transmitted / Input Power (3.3)

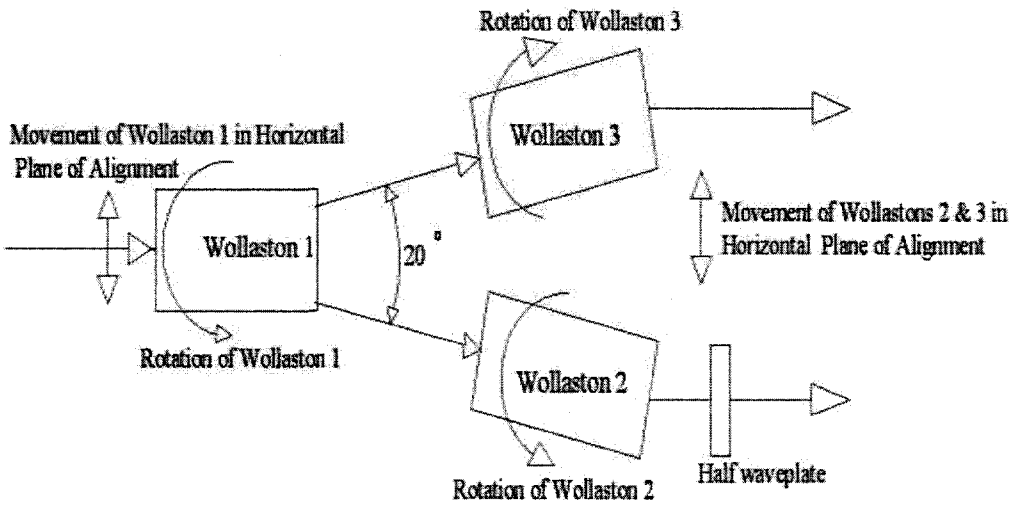

Fig.3.8 Alignment of Wollaston prism

Alignment of the first Wollaston is shown in fig 3.8. The first Wollaston was aligned with respect to the beam position in such a way that maximum power can be achieved transmitted. Maximum transmission efficiency from the first Wollaston was achieved only by aligning the Wollaston in such a way that the laser beam impinges on it orthogonally in the center of the clear aperture. After placing and aligning the first Wollaston, now one quarter waveplate was inserted in the path of the input beam to the first Wollaston to make the polarization of the beam circular.

Transmission efficiency of the first Wollaston was calculated at the wavelength of 1064nm with the help of power meter (Coherent model: LAB MAX TO) after all the alignment was completed with respect to the first Wollaston, input and the corresponding output powers to the first Wollaston were measured at multiple diode current levels and

the transmission power efficiency of the first Wollaston was calculated on the basis of equation (3.3). The transmission efficiency of the first Wollaston was approximately 80%.

3.4.3 Alignment of next two Wollaston prisms

After aligning the first Wollaston and achieving maximum possible transmission efficiency next step was to align the other two Wollaston as shown in the fig.3.8. Beams coming out from the first Wollaston were at an angle of 20^{o} between them and were linearly polarized but with orthogonal in nature with respect to each other. Wollaston two and three were placed just after the output beams of Wollaston one and were aligned in such a way that the output beams from them were straight and parallel with each other with minimum losses. As the input beams to the Wollaston two and three were linearly polarized so output was a single beam. Power was measured after the Wollaston two and three separately and was used for calculating the transmission efficiency. The maximum possible average transmission efficiency achieved from both the Wollaston was approximately 80%.

3.4.4 Alignment of the half wave plate

Laser beam output obtained from the last two Wollastons is linearly polarized but orthogonally with respect to each other. For the interference to happen between two beams polarization of the beams needs to be same in any case. To fulfill this interference

condition polarization state of one of the beams needs to be aligned with respect to the other.

One half waveplate at an angle of 45° was inserted in one of the beam paths for reversing its polarization. Now the basic set up for the machining was set and the distance between the two parallel beams was measured, it was found to be 30mm which was too much for optics that is readily available in most of the optics lab; as commonly available optics usually have optical diameter of 25mm. The output beam spacing cannot be reduced further due to restriction imposed by the size of the Wollaston prisms. The distance between the two parallel laser beam was reduced using focusing optics, so that it can be used with readily available optics therefore installation and maintenance of the setup easier for the industrial application.

3.4.5 Alignment of the distance between the two out put beams

To reduce the distance between the two parallel output beams from Wollaston 2 and 3 some focusing optics was used. First of all one converging lens with focusing length of 500mm and diameter 50mm was placed in front of both the parallel beams for converging the two beams, after converging them for a distance of 300mm a diverging lens of negative focal length of 200mm was used for collimating the two beams again with reduced distance in between them as shown in the fig.3.9. With this pair of converging and diverging lens the beam spacing was reduced to 12mm from 30mm.With different diverging lenses the beam spacing can further be reduced.

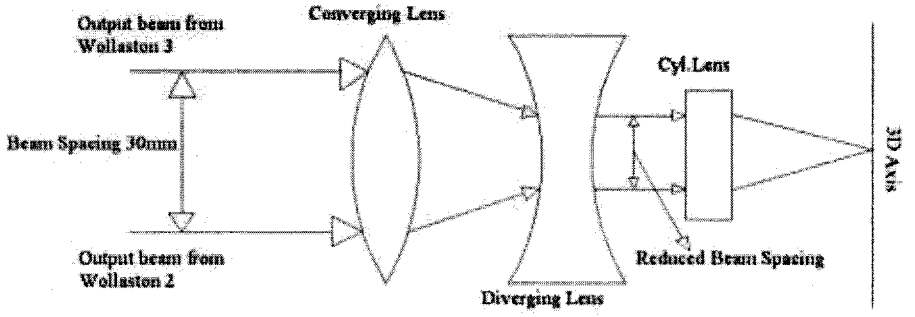

Fig.3.9 Alignment of focusing optics

Some power loses were also associated with the optics used after the second and third Wollastons for aligning the beam spacing. Transmission efficiency of each of the common optics used after the Wollastons being also calculated and the available power at the sample surface for machining was measured.

3.5 Transmission efficiency of common optics

From the following table3.1 it can be seen that some power losses were associated with each optic used in the setup. The average transmission efficiency for most of the optics used in the setup was near to 90% except for cylindrical lens (F=25.6mm) for which it was just 70.8%.the Lower transmission efficiency of cylindrical lens was due to its curvature and thickness. The overall transmission efficiency of the setup was near to 55% with all the optics involved whereas with cylindrical lens (F=25.6mm) it was around 40%.

S.No.	Description of optics	Average transmission efficiency (%)
1	Wollaston Prism	82.48
2	Converging Lens (F=500mm)	92.05
3	Diverging Lens (F= -200mm)	90.35
4	Diverging Lens(F= -150mm)	91.34
5	Diverging Lens (F= -100mm)	94.15
6	Cylindrical Lens (F=100mm)	92.39
7	Cylindrical Lens (F=50.8mm)	90.67
8	Cylindrical Lens (F=25.6mm)	70.80

Table3.1. Transmission efficiency of optics used in the machining setup

3.6 Refinements

Once all the optics included in the setup was aligned with respect to power and position of the beam, then some refinements were done on the setup before the start of final machining experiments. For getting perfect interference while machining at the sample surface, the aim was to focus both the parallel laser beams at a common point on the stainless steel sample.

Some sample machining was done on the stainless steel plate and viewed on the microscope for the final refinements of the setup. In the first machined spot it was found that the two beams were not focusing at the same point and on the same horizontal axis as well as power of the two beams was different as shown in fig.3.10.

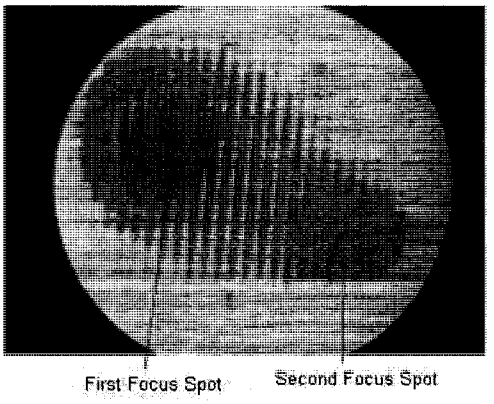

Fig.3.10 Out of plane focusing

Beams were made to align along the same horizontal axis with the rotation of either of the Wollastons two or three as shown in fig.3.8.

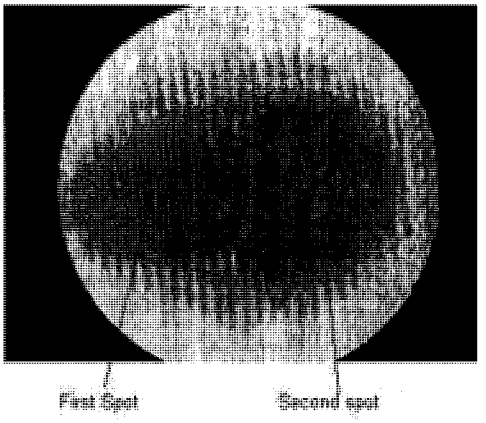

Fig.3.11 In plane different focusing spots

After aligning the two focused spots with respect to vertical axis now again second sample spot was machined on the stainless steel sample. From the microscopic image as shown in fig.3.11 it can be said that still the two spots were out of focused with the horizontal axis or in other words the two beams were not perfectly parallel with each other, due to which the two beams were not focusing at a common point. For refining the

defect the position of the Wollastons two and three were again slightly changed in the horizontal plane in such a way that the out put beams become perfectly parallel.

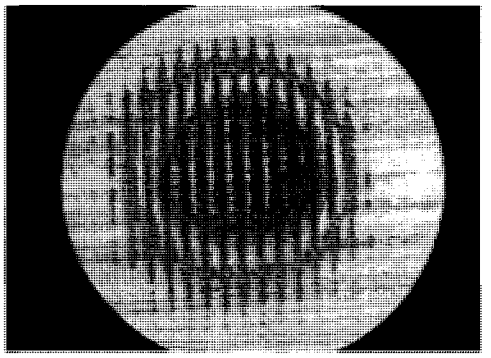

Fig.3.12 Machined spot after all the alignments.

After all these refinements a third spot was machined on the sample surface. From the microscopic image shown in the fig.3.12 it can be concluded that the setup is now perfectly aligned for the final experiments.

3.7 Summary

The setup designed and aligned for the machining was a simple setup for creating interference fringes at the focal point. Amplitude division was achieved with the Wollaston prisms for creating two coherent light beams. Major advantages associated with this setup were that the common optics can be used with this setup as the spacing between the two parallel beams can be easily varied by changing the diverging lens. Transmission efficiency of the setup was more then 50% with all the optics used. Power available at the machining surface was good enough to machine most common metals.

Chapter4

Optimization of Laser Parameters

4.1 Introduction

Experiments for the marking of the contact eye lens inserts were done in two separate parts. In the first part of the experiments effect of different laser parameters on machining stainless steel were studied along with the effect of different focusing lenses and beam spacing. Experiments were done with different laser power, rep. rate and with different machining times, details of all the laser parameters are given in appendix 2. For each new parameter a separate spot was machined and it was characterized with the help of optical microscope and scanning electron microscope.

4.2 Influence of laser power

Laser power is one of the important parameters for the laser marking of the contact eye lens inserts. For studying the significance of laser power on the marking of the stainless steel spots were marking was done with different power levels with all other laser parameters e.g. rep. rate, machining was kept constant. Focusing lens used for the experiments was cylindrical 100mm. Machining was done at three different peak pulse power levels low (6-10) kW, medium (10-14) kW and high (14kW and above). For each power level of laser a separate spot was machined on the stainless steel sample. First spot was machined at a peak pulse power of 8.2kW, second at 11.825 kW and the third at the

20.4 kW respectively. Term available peak power is used to indicate that it was the power available at the surface of the machining samples after considering all the alignment and reflection losses on successive optics as mentioned in table 3.1.

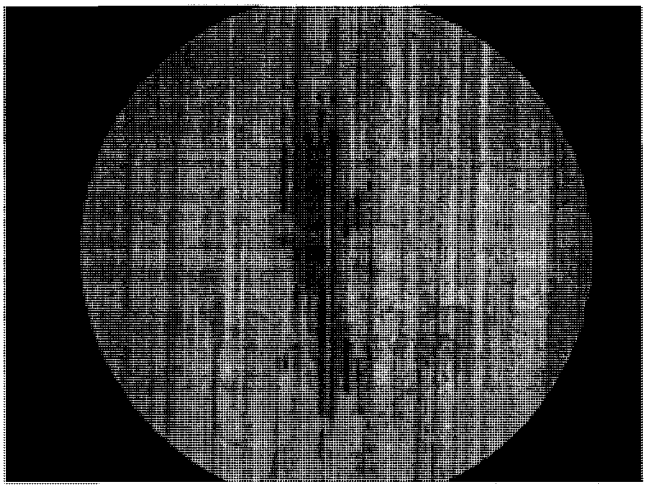

(a)

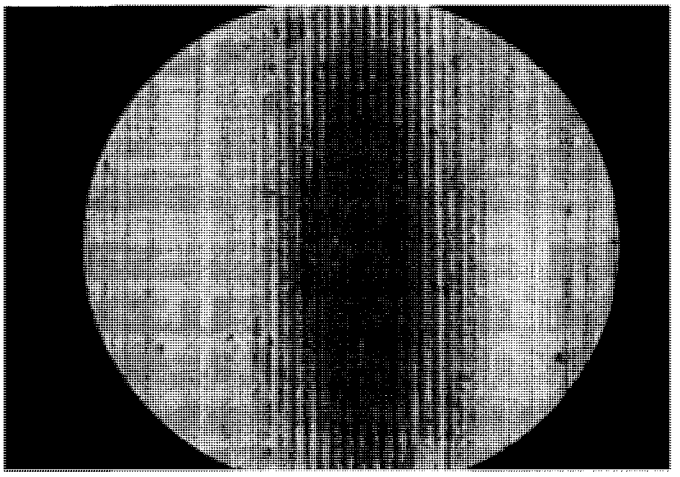

(b)

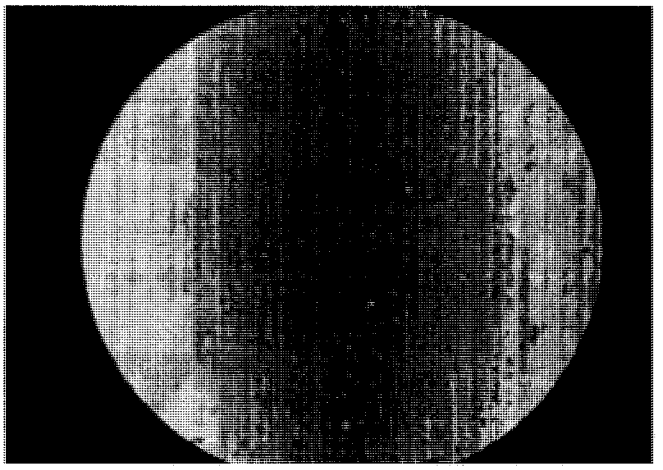

(c)

Fig. 4.1 Spot machined with 20 kHz rep rate, machining time 10seconds (a) 8.2kW of peak pulse power (b) 11.825 kW of peak pulse power(c) Spot machined with 20.4kW of peak pulse power.

Fig.4.1 (a) belongs to the spot machined at a peak pulse power of 8.2 kW whereas fig.4.1 (b) and (c) belong to the spots machined at peak pulse power of 11.2 kW and 20.4kW respectively. From the fig.4.1 it can be concluded that with the increase in laser power the focused spot size of machined surface on the stainless steel surface increases. Also with the increase in the laser power heat affected zone increases which damages the central portion of the machined spot. The machined spot shown in fig.4.1 (a) has less heat affected zone in comparison to machined spots in fig.4.1 (b) and (c); whereas the spot in fig.4.1(c) has the maximum heat affected zone. Increase in the machined spot at higher laser power was because of the Gaussian distribution of intensity, which was predicted and discussed earlier in the theoretical modeling. The experimental results shown in fig.4.1 were compared with the theoretical results in table 4.1 and then the results were plotted on fig.4.2.

S.No	Average Pulse Power (watt)	Focused Spot Size Theoretical(μm)	Focused Spot Size Experimental (μm)	Deviation %
1	4.7	110	100	9
2	6.6	140	130	7.14
3	8.3	166	155	6.2
4	9.6	170	161	6
5	10.4	175	168	5.71

Table. 4.1 Comparison of experimental values with the theoretical

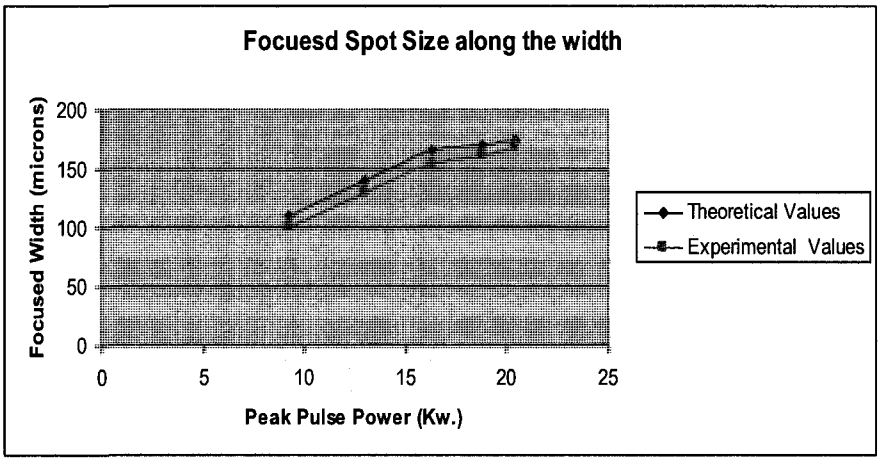

Fig.4.2 Comparison of experimental vs. theoretical values

From the fig.4.2 it can be concluded that the theoretical and experimental values were approximately same and the deviation in the theoretical and experimental vales are due to the losses associated with reflection and other material properties which cannot be exactly simulated on the MATLAB calculation. MATLAB coding was used to calculate the theoretical values (MATLAB coding is attached in appendix 3).

For the better understanding of the machining within the spot, different regions of the same spot were studied. The spot considered for the discussion was machined at 9.2kW of available peak power.

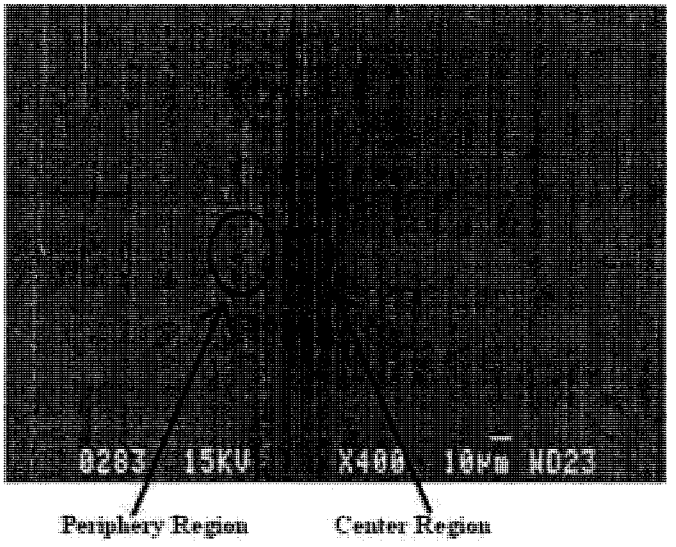

(a)

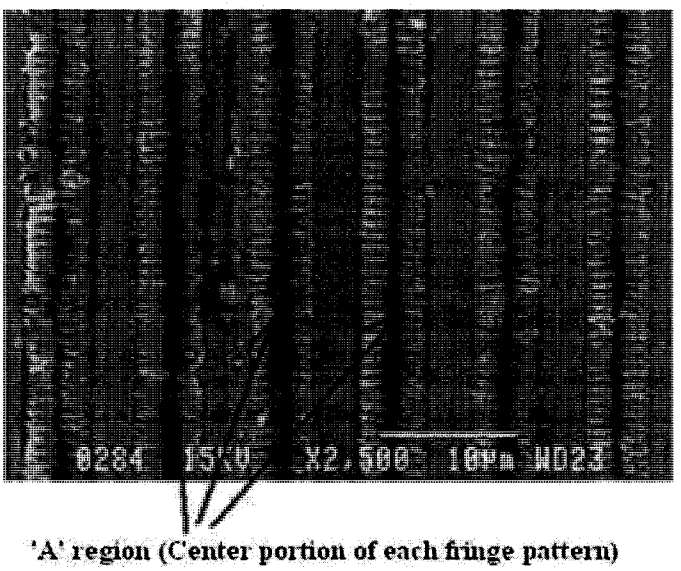

(b)

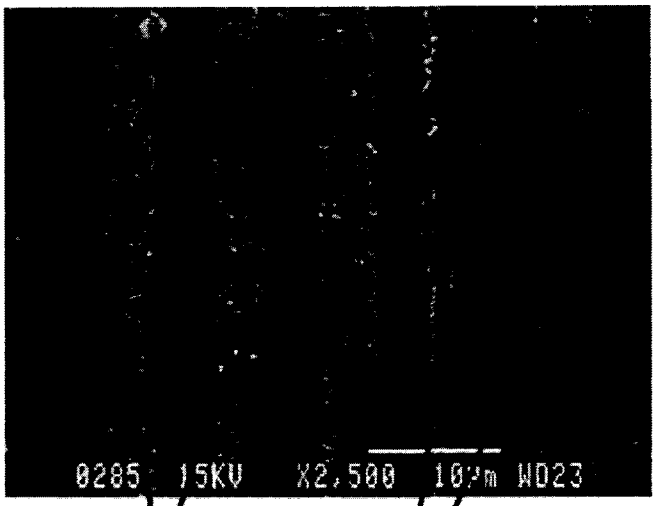

(c)

Fig.4.3 Spot machined at 9.2kW peak power, 20 kHz rep rate and for machining time of 10 seconds (a) Whole spot (b) Center region of the spot (c) Periphery region of the spot

In fig.4.3 different regions of the same spot are shown. In fig.4.3 (b) the fringe patterns shown have black central region in each machined pattern (marked as A region in the SEM picture) which corresponds to the heat affected zone present in the central portion; whereas in fig.4.3(c) which corresponds to the left periphery region of the machined spot, only few fringe patterns have the same black central zone in the machined grating. It means that the patterns which were near to the central portion of the machined spot have more heat affected zone on the other hand patterns far away from the center does not have much heat affected zone present in them. The difference in the heat affected zone and quality of the patterns machined within a single spot was due to the Gaussian intensity distribution as discussed in the theoretical modeling.

Separate experiments were conducted for studying the variation in the depth of the machined spot with respect to different power levels.

(a)

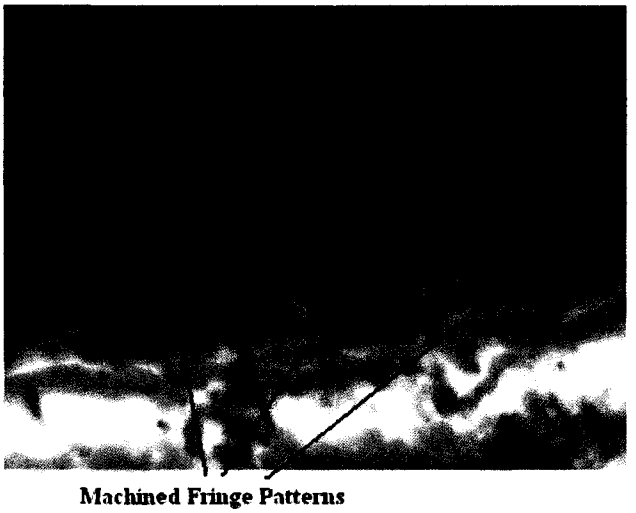

(b)

Fig.4.4. Depth of machining at 20 kHz rep rate (a) 5 μm depth of fringe Pattern at 15kW peak pulse power, (b) 8.5 μm depth of fringe pattern at18.8kW peak pulse power

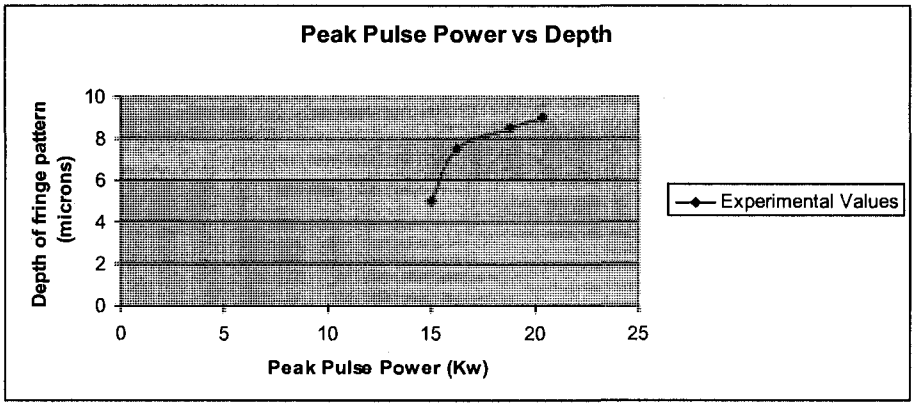

Fig.4.5 Experimental Values of depth with respect to different peak pulse power

As the microscopic images do not have good contrast so the machined region with depths were marked with the dark lines so that it can be distinguished from the un-machined portions. From the fig.4.4 and fig. 4.5 it can be concluded that depth of machining increases with increase in peak pulse power and the machining depth follows a sinusoidal profile which is clearly evident and explained with the interference principle in theoretical modeling. From the plotted experimental values in fig 4.5 it can be easily concluded that slope of the plot was high at low peak pulse power but the slope was low at high power levels which indicates a saturation level of depth with respect to power after certain level. Depth of the central fringe pattern was 5 μm when machined with available peak pulse power of 15kW, and depth of machined fringe pattern increases to 8.5μm with an increase of available peak pulse power to 18.8kW. Central fringe have maximum depth in all the machined fringes due to Gaussian beam intensity distribution. For all the depth calculations central fringe was used. From these experiments at multiple power levels it can be concluded that for achieving the depth of marking in the range of 5-15 μm the peak pulse power of the laser has to be kept in between 14kW to22

kW . Also for better quality of the marking with the desired width of 10- 20 μm as discussed in the objective the laser power will also remain in the same range of 14kW to22 kW.

4.3 Effect of repetition rates

Rep. rate is the other important parameter of the pulsed laser from marking point of view. The Nd: YVO4 laser used for the experiments can be tuned for different rep rates starting from 20 kHz to 100 kHz .Multiple spots were machined at different rep. rates with constant laser power and machining time as mentioned in design of experiments in appendices 2.

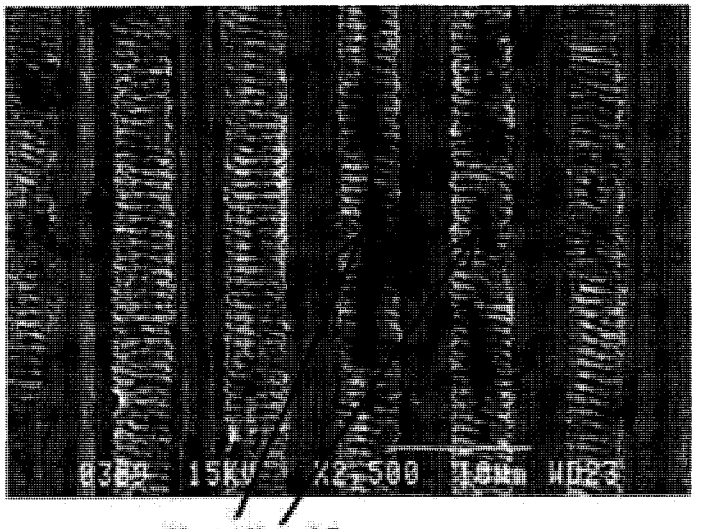

(a)

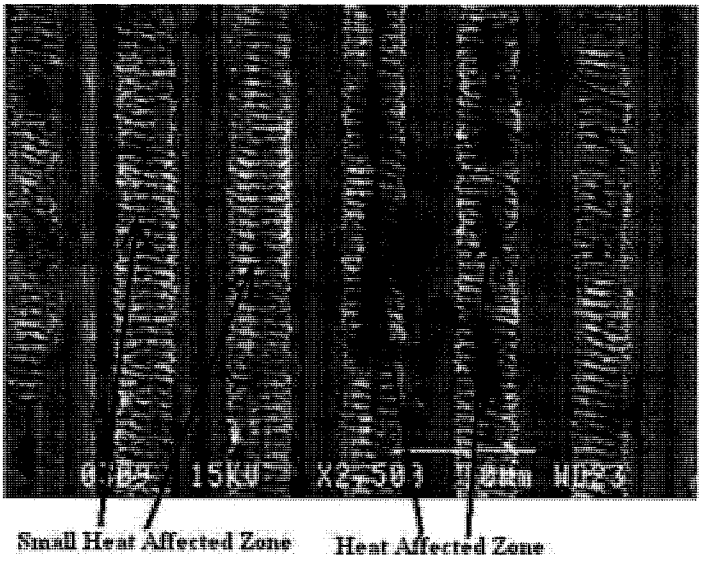

(b)

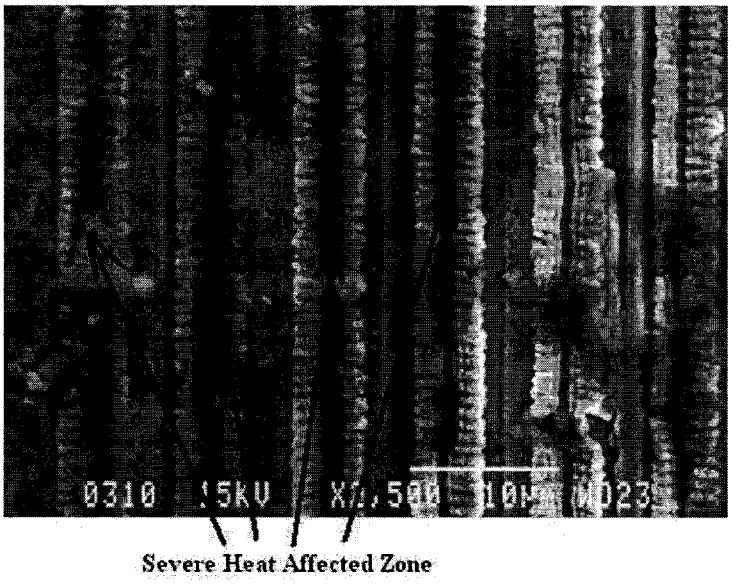

(c)

Fig.4.6 (a) Spot machined with rep rate of 40 kHz, peak pulse power of 14.73kW (b) Spot machined with rep rate of 30 kHz, peak pulse power of 9.035kW (c) Spot machined with rep rate of 20 kHz, peak pulse power of 6.38 kW

In fig.4.6 focused spots machined with different rep rates are shown. From the images of the fig.4.6 it can be concluded that the machining done at 40kHz have less heat affected zone in comparison to the machining done at 20 and 30kHz of repetition rates. The heat affected zone was severe or maximum for the spot machined with 20 kHz of rep rate as shown in fig.4.6(c).These results are according to predicted results of the theoretical modeling. Theoretical modeling was done with respect to equation (4.1) which gives energy per pulse with respect to average power and repetition rate.

$$\textit{Energy per pulse (Joules)} = \textit{Power average (watt)/ Rep. Rate (KHz)} \qquad (4.1)$$

From the laser system chart supplied by the Coherent laser it can be seen that with the increase in the rep rate from 20 kHz to 30 kHz the average power of the laser increases from 6.6 watts to 6.9 watts. The increase in the laser power is very small in comparison to the increase in the rep rate and from the equation (4.1) it can be easily calculated that with the increase in the rep. rate the energy per pulse (peak pulse power) will decrease, the calculation for peak pulse power with different rep rate was shown in the previous chapter of theoretical modeling. This decrease in the pulse energy was clearly evident from the less heat affected zone present in the machined spot of 40 kHz rep rate.

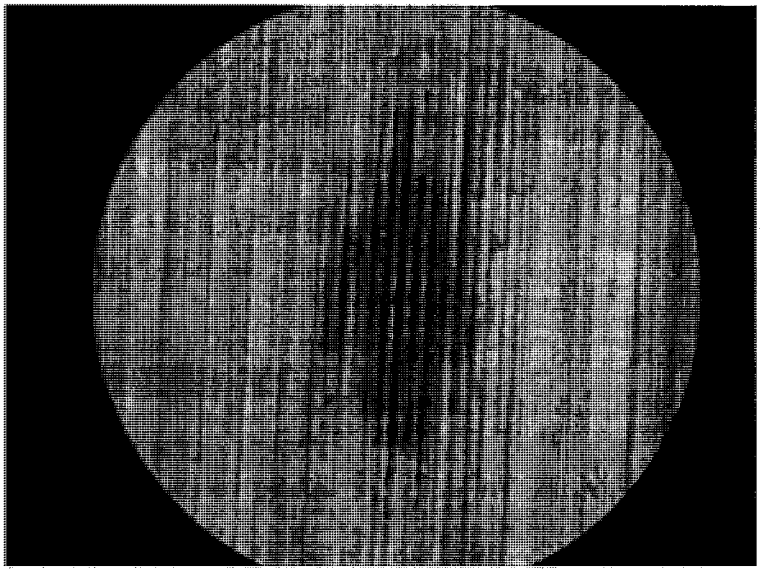

(a)

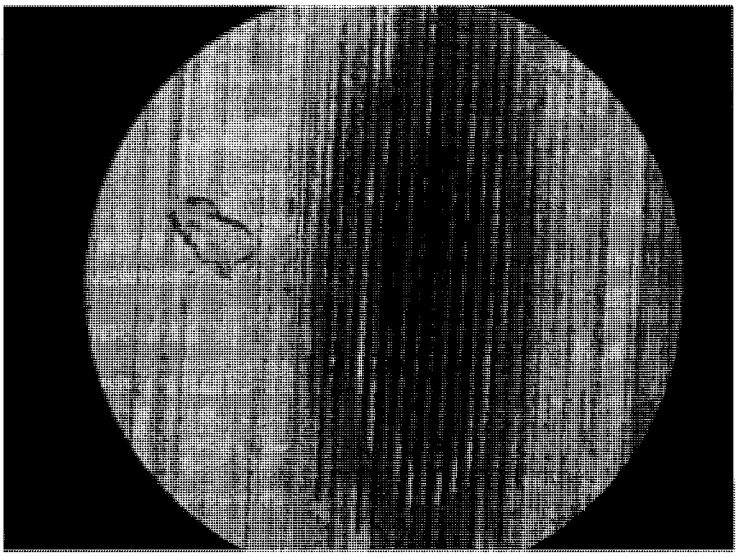

(b)

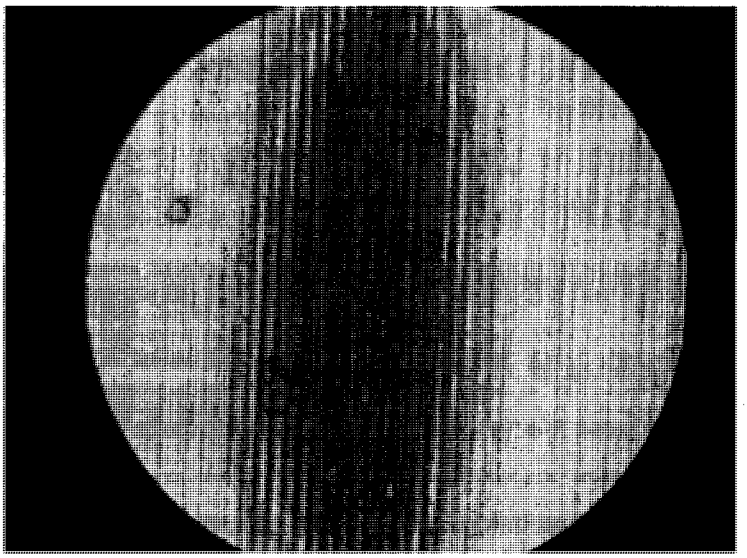

(c)

Fig.4.7 (a) Spot machined with rep rate of 40 kHz, peak pulse power of 14.73kW (b) Spot machined with rep rate of 30 kHz, peak pulse power of 9.035kW (c) Spot machined with rep rate of 20 kHz, peak pulse power of 6.38 kW

From the fig.4.7 it can be concluded that with the increase in rep rate the spot size decreases. This decrease in the machined focused spot size was due to the decrease in peak pulse power with increased rep rate. Theoretical results for machined spot along the focused portion of the spot were compared with the experimental results of fig.4.7 and were plotted in fig.4.8 for the comparison.

S.No	*Rep Rate (kHz)*	*Focused Spot Size Theoretical(μm)*	*Focused Spot Size Experimental (μm)*	*Deviation %*
1	*20*	*140*	*130*	*7.14*
2	*30*	*130*	*122*	*6.16*
3	*40*	*120*	*110*	*8.33*

Table. 4.2 Comparison of experimental values with the theoretical

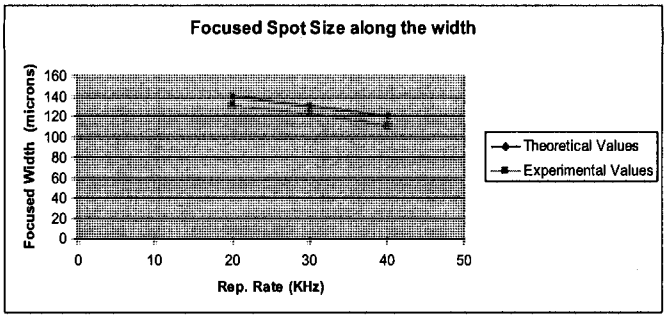

Fig.4.8 Comparison of theoretical and. experimental Values for different rep rates.

From the fig.4.8 it can be said that that experimental results were close to the theoretically calculated values. The deviation shown in the experimental and theoretical values were due to the reflection losses from the surface as well as from the other successive optics as discussed in previous section.

Now it can be concluded with these experiments that with the increase in the rep rate energy per pulse will be decreased which reduces the heat affected zone and increases the quality of the machined fringe patterns as evident from the fig.4.6 and fig.4.7 .For better quality of the patterns with minimum heat affected zone on the lens inserts the rep rate has to be kept around 40kHz, as no significant amount of machining took place above 40kHz of rep rate.

4.4 Variation in depth with different variation in number of pulses hitting the surface

For studying the effect of different number of pulses on the machining depth; experiments were conducted with stainless steel sample on a moving stage. Laser system

used for the experiments does not have any provision of controlling the number of pulses coming out from the laser head. With different speed of the moving stage the number of pulses hitting the same region can be varied. Stainless steel sample was kept on the moving stage and machining was done with different feed rates of the stage. At higher feed rates less number of pulses will hit the same surface whereas at low feed rates the machining was done with higher number of pulses hitting the same region again and again. If for example the length of the machined spot is 400 μm and speed of the moving stage is set at 100 μm/second and machining will be done with 20kHz rep rate then the number of pulses hitting the same region during the moving stage will increase to 4 times and 80kHz pulses will hit the spot, as sample will move only one forth the distance of the length of the spot during the specified time.

(a)

(b)

Fig.4.9 Machining done at peak pulse power of 18.85kW (a) Depth of machining is 7 μ at 0.1 μ/sec feed rate, (b) Depth of machining 16 μ at 0.01 μ /sec feed rate

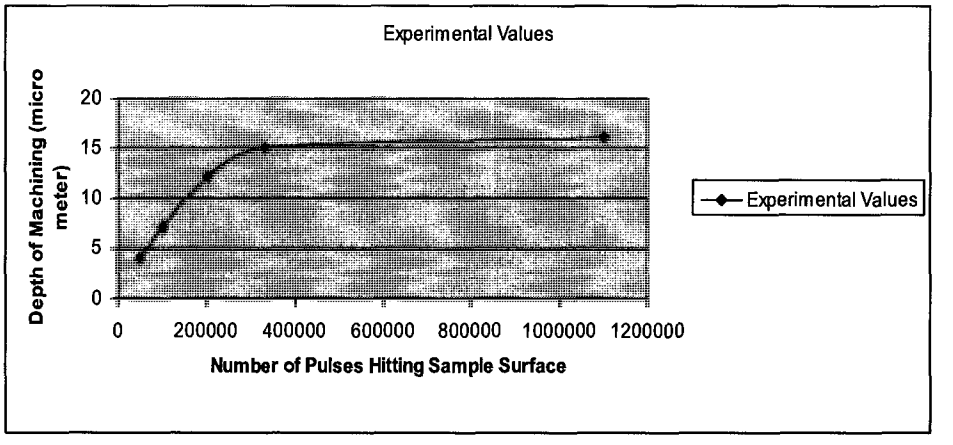

Fig.4.10 Experimental values for the depth of machining at 18.85kW of peal pulse power and different feed rates of the stage.

In fig.4.9 optical microscopic images of machining are shown, whereas in fig.4.10 different marking depths are shown with respect to different number of pulses

hitting the surface. From the fig.4.9 and fig.4.10 it can be concluded that the depth of machining increases with increase in the number of pulses hitting the same region up to certain level and after that a saturation level was reached and increase in depth with increase in number o pulses was negligible. Machining done with lesser number of pulses has well defined depth for each fringe, whereas quality of the machined patterns reduces significantly with higher number of pulses due to high heat affected region and material re-deposition as shown in fig 4.11. The reduction in quality of the patterns is attributed to the more conduction of heat in the machining region due to increased machining time.

Number of pulses hitting the surface can also be controlled with different machining times. Increase in the machining time increases the number of pulses hitting the surface and vice versa. In this part of experiments the machining time was varied keeping all other laser parameters e.g. rep. rate and power constant.

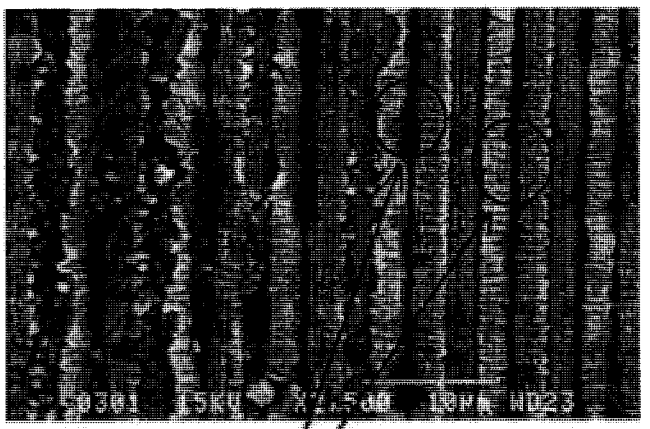

(a)

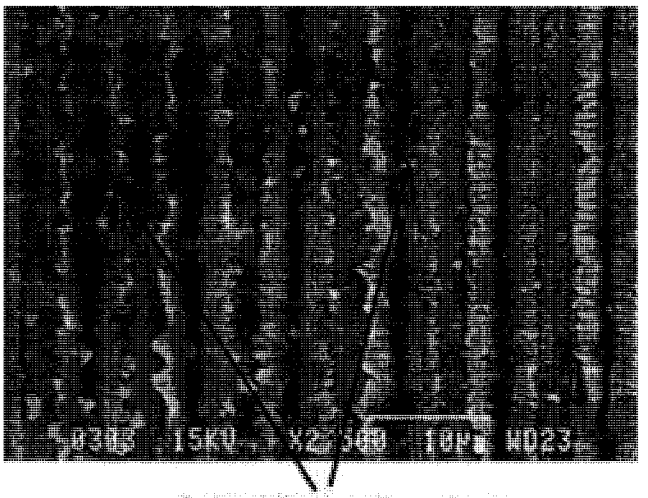

(b)

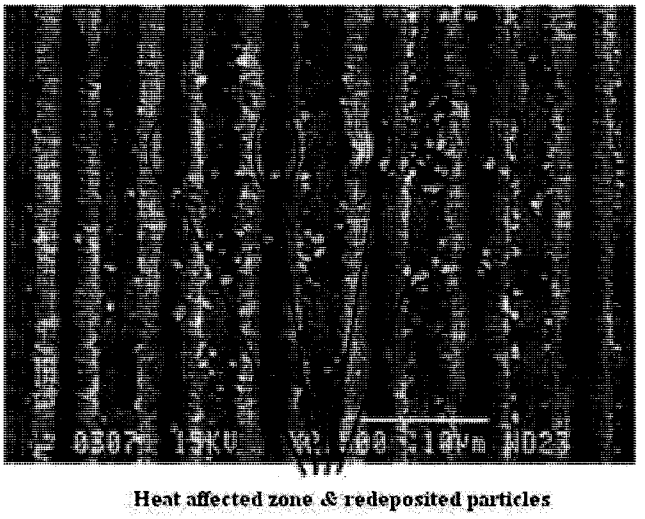

(C)

Fig. 4.11 Machining done with 20kHz rep rate,9.23kW peal pulse power and for machining time of (a) 5 seconds (b) 15 seconds (c) 25 seconds

In fig.4.11 SEM images were shown for spots machined with 5sec, 15sec and 25 seconds of machining time respectively. From fig.4.11 it can be concluded that with the increase in machining time heat affected zone increases, which is evident from the image

fig.4.11(c) in which the patterns machined were of bad quality due to the heat affected zone in each grating in the center; whereas the patterns machined with lesser machining time does not have much heat affected zone as shown in fig.4.11 (a).

4.5 Summary

From the experimental results related to various laser parameters it can be summarized that the quantity and the quality of the laser based marking of stainless steel depends significantly on laser parameters e.g. power, rep.rate and machining time. Optimum level of laser parameters is required for machining high quality of patterns on the stainless steel lens inserts. Optimum peak pulse power (9.7 kW) is required to machine the required number of patterns with desired marking depth of 5-10 μm, with very low power (6 kW) number of patterns machined within the spot size will be restricted on the other hand if machining is done with very high power (19 kW) number of patterns will be increased but the patterns in the center portion will be damaged. Similarly with the increase in machining time the quality of the pattern will drop significantly due to increase in the heat affected zone.

Chapter 5

Optimization of optical setup

5.1 Introduction

As mentioned in the previous chapter that experiments was conducted in two parts. In first part of experiments effect of laser parameters were discussed with respect to quantity and quality of machining stainless steel. Marking done on inserts will finally come on the external surface of the toric eye lens. Experiments were done to vary the pitch of the machined patterns with respect to focusing lens and beam spacing. Experiments were also done with different state of polarization.

5.2 Variation in the pitch of the fringe patterns

Pitch between the fringe patterns can be changed with the variation in the angle theta (θ) between the two focusing beams at the focus as shown in the fig. 5.1 where Z was the distance between the two parallel beams and F was the focusing length of the lens.

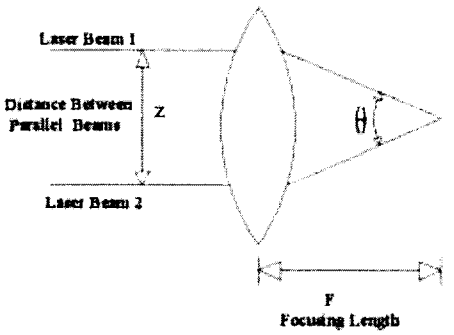

Fig.5.1 Focusing beam with beam spacing Z and focusing lens F [56]

$$\text{Pitch} = \lambda/2\text{Sin}(\theta/2) \tag{5.1}$$

$$\theta/2 = \tan^{-1}(Z/2F) \tag{5.2}$$

From the equations 5.1 and 5.2 it can be seen that the angle theta (θ) is a function of focusing length of lens (F) and beam spacing (Z) between the parallel laser beams. [56].

5.2.1 Variation in pitch with different beam spacing

Experiments were conducted with three different beam spacing of 6mm, 9mm and 12mm with a constant focusing length of 100mm. For each beam spacing one separate spot was machined on the stainless steel sample which was further characterized for the pitch with the help of scanning electron microscope. Pitch of the gratings obtained from the experiments was compared with the theoretical pitch value obtained from the equations (5.1) and (5.2).

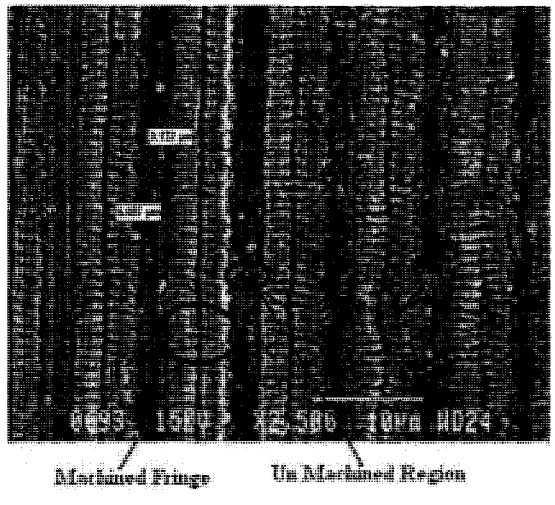

(a)

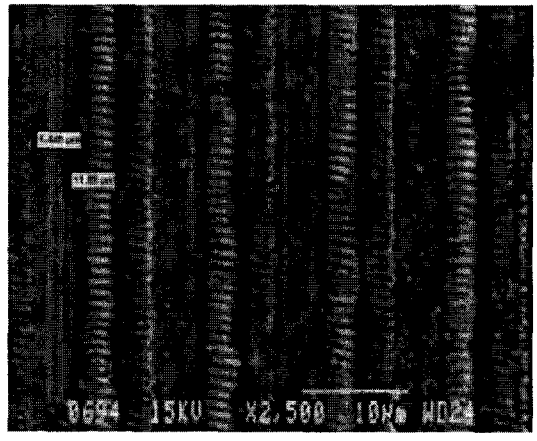

(b)

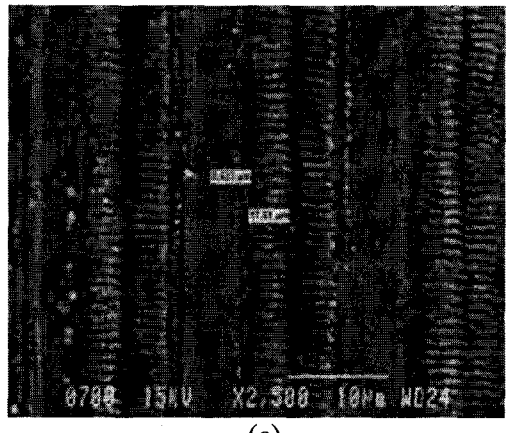

(c)

Fig.5.2Fringe patterns machined at rep rate of 20kHz,machining time of 10 seconds, peak pulse power of 15.12kW with a (a) beam spacing of Z=12mm, (b) beam spacing of Z=9mm (c) beam spacing of Z=6mm

S.No.	*Beam Spacing(mm)*	*Theoretical Values(μm)*	*Experimental Values(μm)*	*Deviation (%)*
1	*6*	*17.83*	*17.61*	*1.2*
2	*9*	*11.83*	*11.88*	*0.42*
3	*12*	*8.668*	*9.132*	*5*

Table 5.1 Comparison of experimental pitch with theoretical pitch

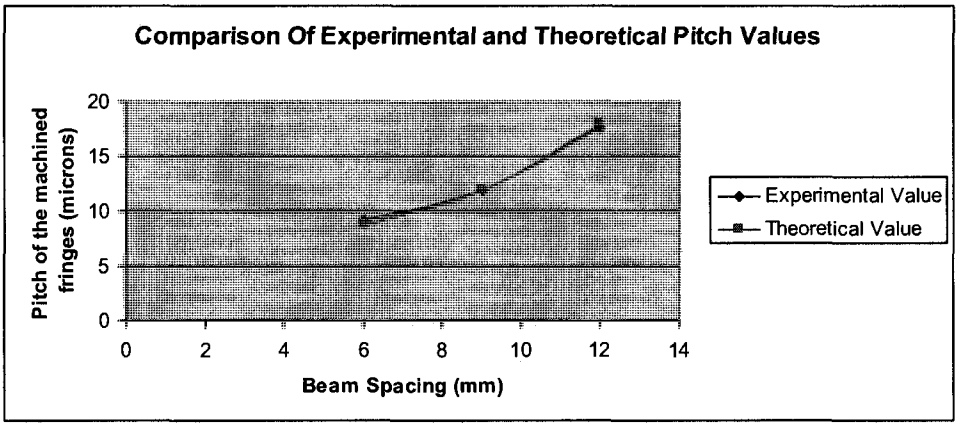

Fig.5.3 Comparison of theoretical and experimental pitch values

Fig.5.3 shows that the variation in pitch with respect to beam spacing was according to the given theory. The small variation in the experimental and theoretical values was due to the limitation of measuring the beam spacing manually in the lab. It can be concluded from the experimental as well as theoretical results that pitch of the grating can be increased with decrease in the beam spacing which is one of the advantages of the proposed optical setup.

5.2.2 Variation in pitch with different focusing lens

As discussed in the previous section that pitch of the fringe patterns can be changed either, by changing beam spacing or by changing focusing lens. In this part of the experiments different focusing length lens were used for machining the stainless steel sample and the results obtained for the pitch were compared with the theoretical pitch values.

Experiments were done with a beam spacing of 7mm and with three different focusing lenses of 100mm, 50.8mm and 25.6mm.Beam Spacing was kept at 7mm so that that the gratings can be separately characterized even with shorter wavelengths otherwise for higher beam spacing it is almost impossible to separate the patterns machined with shorter focal lengths of 25.4mm. Machined spots were characterized with the help of scanning electron microscope.

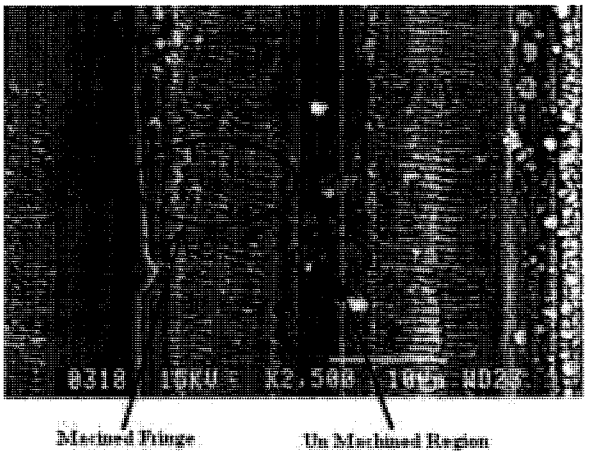

(a)

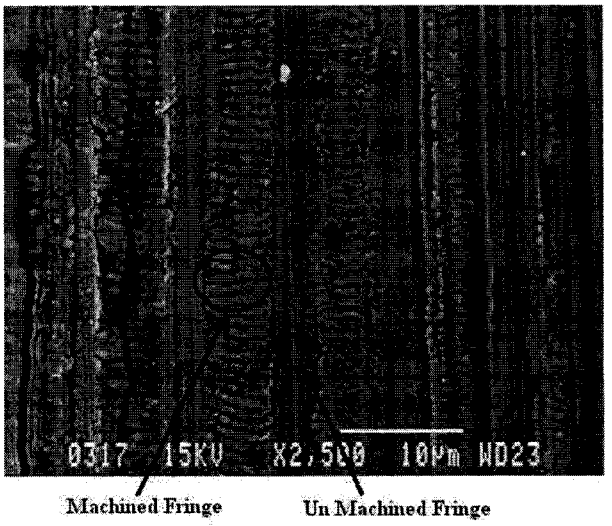

(b)

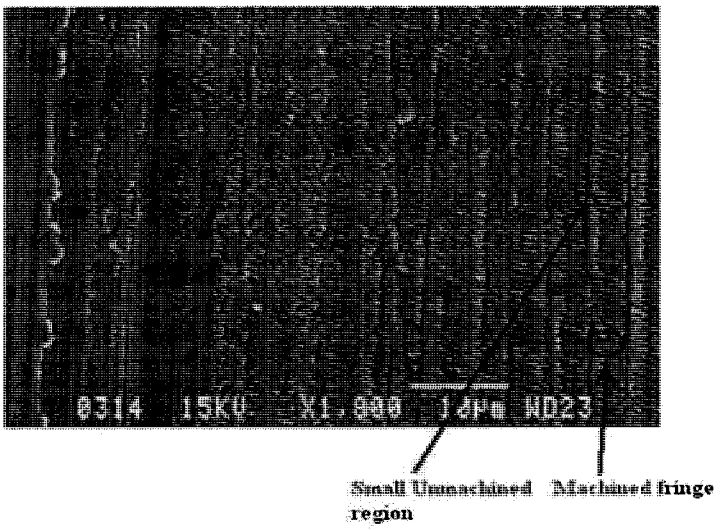

(c)

Figure 5.4 Fringe patterns machined at rep rate of 20kHz,machining time of 10 seconds, peak pulse power of 15.12kW with a (a) focusing lens of F=100mm (b) focusing lens of F=50.8 mm (c) focusing lens of F=25.4 mm

Pitch obtained with a focusing lens of 25.4mm is smallest in comparison with the pitch obtained with 50.8mm and 100mm focusing lenses, whereas the pitch obtained with the 100mm focusing lens is largest in all the three pitch values. The spacing between the fringe patterns machined with focusing lens of 25.4mm in fig.5.4(c) were very close that even it was not possible to distinguish between the two patterns in the center but in the right corner some patterns were slightly distinguishable. These results were compared with the theoretical results and the results were plotted in fig.5.5.

S.No	Focusing Length(mm)	Theoretical Values(μm)	Experimental Values(μm)	Deviation (%)
1	100	15.2	16.0	5.2
2	50.8	7.74	8.0	3.3
3	25.4	3.89	4.0	2.8

Table 5.2. Experimental and theoretical values of pitch

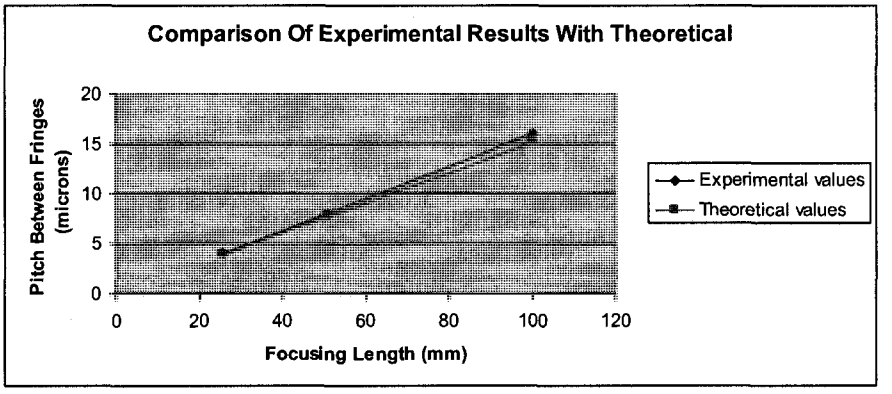

Fig5.5 Comparison of Experimental and Theoretical results

From the fig.5.4 and fig.5.5 it can be concluded that the minimum possible pitch that can be obtained with the experimental setup was approximately 3 μm, also it is difficult to separate two machined fringe patterns if the focusing length was low.

Pitch can be easily varied with the help of focusing lens, for higher values of pitch machining has to be done with higher focusing lens and for smaller pitch values machining has to be done with lower focusing lens.

5.3 Number of fringe patterns machined

In the proposed marking method the machined fringe patterns transferred on the toric lens surface can also be used as grating element. Number of fringe patterns formed on the inserts is also an important parameter of marking and needs to be controlled during the marking process. Number of fringe patterns machined on the lens inserts can be controlled by the control of peak pulse power. As discussed earlier in theoretical modeling the number of fringe patterns machined on the lens inserts can be increased by increasing the peak pulse power or can be decreased by decrease in peak pulse power. In first set of experiments peak pulse power of the laser pulse was varied with average pulse power of the laser. Experimental results were compared with the theoretical results and were plotted in fig.5.6.

S.No	*Peak Pulse Power (kW)*	*No. of gratings created theoretical(μm)*	*No. of gratings created Experimental (μm))*	*Deviation %*
1	*9.2*	*17*	*16*	*5.8*
2	*12.96*	*19*	*18*	*5.26*
3	*16.3*	*21*	*20*	*4.7*
4	*18.8*	*22*	*21*	*4.5*
5	*20.4*	*22*	*21*	*4.5*

Table 5.3 Number of fringe patterns with different average pulse power

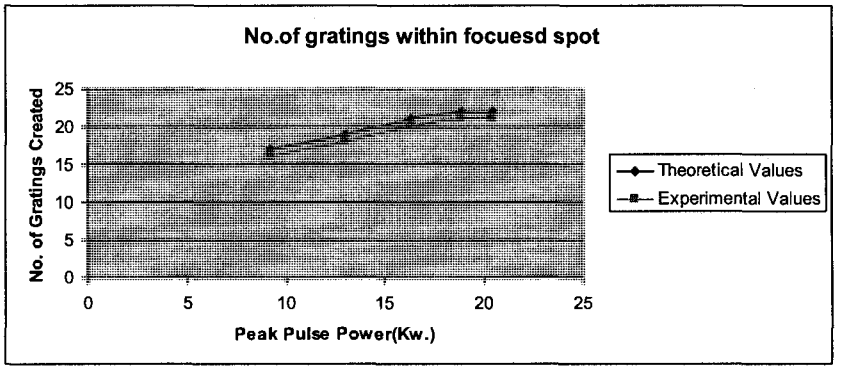

Fig.5.6 Comparison of theoretical and experiments results

From the fig.5.6 it can be concluded that with the increase in peak power the number of fringe patterns machined on the insert was increased, but slope of the curve between number of patterns and peak pulse power is steeper for lower values then for higher values which indicates that increase in the machined patterns with peak pulse power was more at lower range (10-15kW) of the curve with respect to increase at higher peak values (15 kW and above).Peak pulse power can also be varied by the change in rep rate as discussed in theoretical modeling. Theoretical results were compared with the experimental values and were plotted in fig.5.7.

S.No	*Rep Rate (kHz)*	*No. of fringes created Theoretical(μm)*	*No. of fringes created Experimental (μm))*	*Deviation %*
1	*20*	*19*	*18*	*5.26*
2	*30*	*17*	*16*	*5.88*
3	*40*	*14*	*13*	*7.14*

Table 5.4 Number of fringe patterns with different rep rate

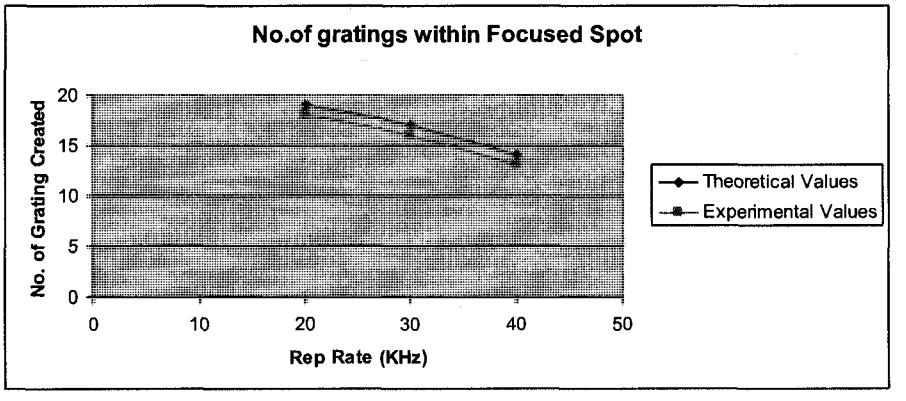

Fig.5.7 Comparison of experimental values with theoretical

From the fig.5.7 it can be concluded that with increase in rep rate the number of fringe patterns machined will decreases whereas at lower rep rates more patterns were machined.

5.4 Machining with different set of laser polarization

Experiments were done with different laser parameters (e.g. pulse power, rep rate and time of marking) to study the affect of each parameter on the marking quantity and quality. From all the scanning electro microscope images it can be seen that there were some regularly arranged patterns in each fringe pattern. Explanation for these ripple patterns were given by several researchers in their published works. In the research papers [85-87] it was explained that these ripple patterns are due to the interference between the incident lasers light and scattered or diffracted light parallel to the sample surface. Microscopic roughness of the sample surface, small defects and spatial variations in the dielectric constant of the sample surface was stated as the region for scattering of the incident light. The pitch of these ripples depends on the polarization, wavelength and angle of incidence of the laser beam with the surface. The orientation of the ripples is determined mainly by the polarization of the laser beam. The ripples are mainly oriented perpendicular to the electric vector of the laser beam and if the laser beam is circularly polarized than ripple patterns will follow random patterns [88].

To obtain better quality with respect to polarization of laser beam, experiments were done on stainless steel samples with different laser beam polarization and the results

were compared with each other as well as with the preciously published work of other researchers.

Beams coming out from the Wollaston 2 and Wollaston 3 were linearly polarized but their polarization direction was orthogonal to each other as already discussed in the chapter of experimental setup. As, discussed earlier one half wave plate was used to maintain the same polarization between the two beams.

Experiments were done first by inserting the half wave plate in the path of beam coming out from Wollaston 2 as shown in fig.5.8.When half waveplate was inserted in the output beam from wollaston 2 then the polarization of the beam was changed and it becomes similar to the polarization of beam coming out from wollaston 3.

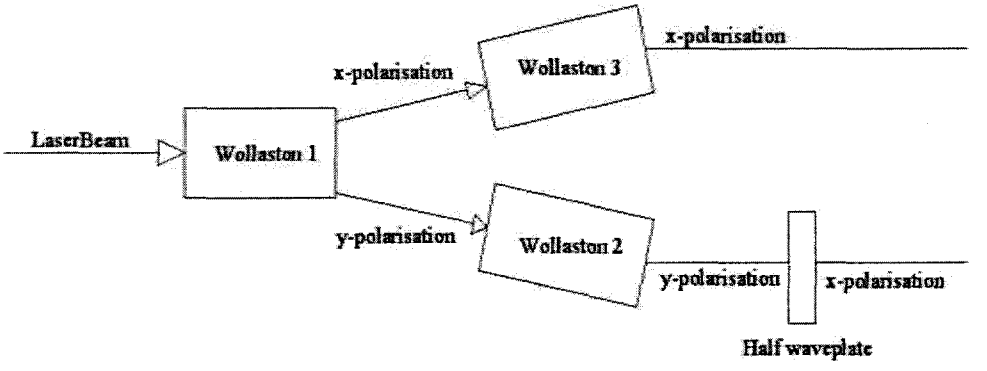

Fig.5.8 change in polarization with Wollaston 2 output

SEM image of the single fringe machined with the above mentioned polarization is shown in fig.5.9.From the images it can be seen that each fringe has some ripple

patterns aligned in one direction. Small ripple patterns ablated within each fringe were perpendicular to the axis of the marking shown in fig.5.9.

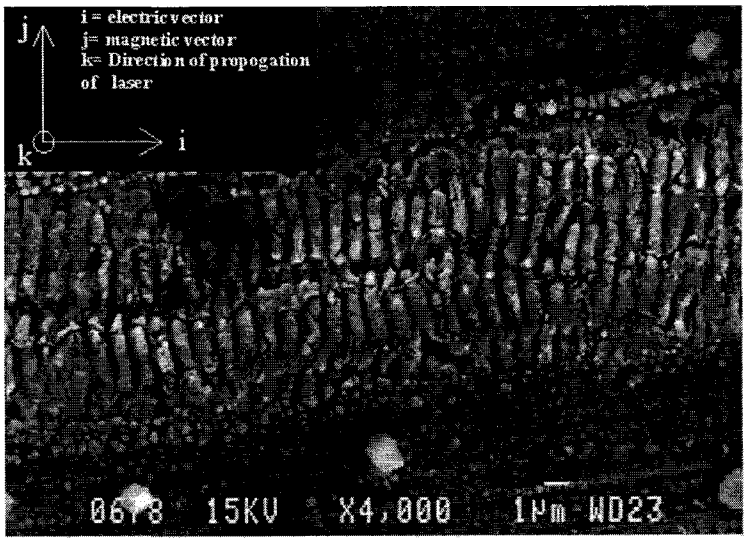

Fig5.9 single fringe machined with x polarization at rep rate of 20 kHz, machining time of 10 seconds and peak pulse power of 15.12 kW

Next Experiments were done by inserting the half wave plate in the output beam coming of Wollaston 3 as shown in fig.5.10.When half waveplate was inserted in the output beam from wollaston 3 then the polarization of the beam was changed and it becomes similar to the polarization of beam coming out from wollaston 2 as shown in the fig.5.10.

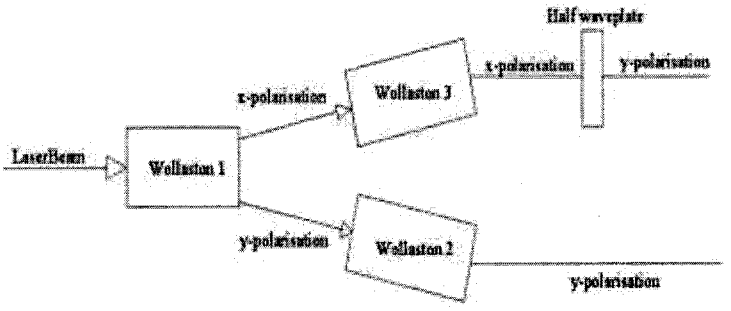

Fig.5.10 change in polarization with Wollaston 3 output

SEM image of the single grating machined with the above mentioned polarization is shown in fig.5.11. From the small patterns machined within a single fringe, direction of the polarization can be analyzed. Small patterns ablated within fringe as shown in fig.5.11 were parallel to the axis of the fringe. The direction of these patterns must be perpendicular to the electric vector which means that the polarization vector of the laser beam was perpendicular (s-polarization) to the fringe axis as explained earlier [88].

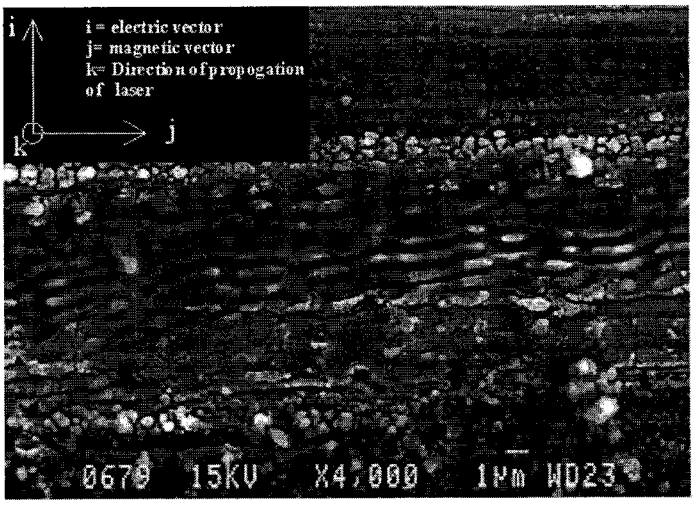

Fig5.11 single fringe machined with x polarization at rep rate of 20kHz, machining time of 10 seconds and peak pulse power of 15.12 kW

From the results obtained with different set of polarization it can be concluded that polarization of the laser beam is important for improving the quality of contact lens marking. The ripple patterns formed within each fringe pattern can distort the quality of the marking if, not taken into account properly. To minimize the effect of these ripple patterns direction of patterns parallel to the fringe axis or marking axis are required.

5.5 Summary

Discussion done after these experiments can be summarized by concluding that the pitch of the fringe patterns machined on the contact lens inserts can be easily varied by using different focusing lenses and beam spacing. Pitch of the fringe patterns can be reduced by either reducing beam spacing or decreasing the focal length. Polarization of the laser beam used for marking the toric contact eye lens inserts must be selected in such a way that ripple patterns formed within each fringe will be parallel to the direction of the fringe axis therefore electric vector perpendicular to the fringes are required for the marking purposes.

Chapter 6

Conclusion and Future Work

6.1 Conclusion

Toric contact eye lens marking is critical for proper functioning of the toric lenses. Most of the current marking methods are cumbersome or time consuming therefore the proposed marking method, based on the interference principle has good industrial application for the marking of toric contact eye lenses. With the proposed marking method not only the area of marking will be decreased but also visibility of the marks with slit lamps increase.

Diffrent marking methods are studied in depth with respect to laser marking methods and non laser marking methods.Objective of the research project was set with respect to the past marking methods in such way that it will increase the visibily of the marks with simple marking design based on intereference principle.

Theoretical modeling has been done to predict the nature and region of marking with respect to different marking axis. Modeling has been done to calculate the variation in depth due to the aspehrical profile of the toric lens inserts. From the modeling part it was concluded that variation in depth along the length of the marking is approximately 12 μm and along the width of the marking variation is less than 0.5 μm. Therefore for the continuous marking, depth of marking has to be kept above 12 μm, within a marking length of 1mm. Major advantage associated with the interference based marking is that

half the laser power is required to obtain the same depth as obtained without interference. As the laser power required is reduced to half heat affected zone decreases which significantly improves the quality of marking and increase the life of the metal inserts.

The optical setup designed for the experiments can be used with readily available optics. Due to simple optics and less tedious alignment task the setup can be used in industries for commercial applications with minimum maintenance requirements.

In the first set of experiments different laser parameters e.g. peak pulse power, rep. rate and number of pulses were studied with respect to quality of marking as well as for quality of marking. Medium peak pulse power in the range of (8-10) kW with a rep rate of 30 kHz is required for high quality marking with a marking depth of (8-10) μm. Higher peak pulse power above 12kW and lower rep rates lower than 30 kHz reduced the quality of marking with significant amount of heat affected region and material re-deposition. Marking depth can be increased with increase in number of pulses hitting the surface, but after a certain level of number of pulses the increase in marking depth will not produce change in marking depth and it will only reduce the quality of the marking with increased heat conduction in marking region.

Second set of experiments were mainly done to improve the quality of the marking with respect to polarization and to create variation in marked patterns with respect to different fringe pitch. From the experiments it was concluded that pitch between the two marked fringes patterns can be increased with increase in focusing length or decrease in beam spacing between the two parallel beams and vice versa. From the experiments done with different set of laser polarization it can be concluded that

polarization of the laser beam used for marking the toric contact eye lens inserts must be selected in such a way that ripple patterns formed within each fringe will be parallel to the direction of the fringe axis therefore electric vector perpendicular to the fringes are required for the marking purposes.

6.2 Future Work

In the proposed research project a new marking method based on interference principle has been proposed with stainless steel sample and laser head in a fixed position. Further work can be done with metallic insert on a gimbal mount so that the variation in the marking depth can be compensated with the movement of metal insert according to its aspherical radii of curvature. Fringe patterns obtained on the toric lenses can also be used as diffraction grating if used with slit lamps having white light as a source. On illumination of fringe patterns different orders of gratings can be obtained which will help in locating the axis of toric lenses with respect to eye.

Re-deposition of metal particles during marking with pulse laser can be reduced if marking will be done either in vacuum or under liquid. Marking done under liquid will also reduce the heat affected zone, but the size of marking will be affected due to change of refractive index of medium. Electronic shutters can be used with the laser system for controlling the number of pulses hitting the metal sample.

Reference

1. http://www.contactlensdocs.com/History%20of%20Contact%20Lenses.htm
2. Contact Lens Practice, 3rd Edition, Mandell, R.,B., page 6, Charles C. Thomas, Springfield, IL, 1981.
3. Contact Lenses: The CLAO Guide to Basic Science and Clinical Practice, 2nd Edition, page 1.7, 1989, Little Brown and Company, Boston, MA.
4. Gregory J. Hofmann et. al.;"*Shape memory polymer or alloy ophthalmic lens mold and method of forming ophthalmic products*" US Patent 6827325, *2004*
5. Wayner E. Williams et.al; "*Marking of mold inserts to produce marked contact lenses*" US Patent 5641437 ,*1997*
6. Richard C. Rogers et. al.; "*Contact lens with moulded inversion marks*" US Patent 6568807;*2003*
7. http://www.1-save-on-lens.com/contactsmaterials.html
8. http://www.fta.gov/cdrh/contactlensestypes.html
9. http://intl.elsevierhealth.com/e-books/pdf/259.pdf
10. Encyclopedia on astigmatism
11. Nicolas Chateau et.al.; "*Method of producing angular tolerance marking for lenses for correcting astigmatism and associated lenses*" US Patents 6086202,*2000*
12. William J Appleton, et. al.; "*Toric contact lens markings*" US Patents 6491393; *2002*
13. William J Appleton et.al; "Method for identifying characteristics of contact lenses" US Patents 6079826; *2000*
14. Martin J Drazba et.al; "*Asymmetric contact lens*" US Patents 5062701;*1991*
15. Paul Hahn et al; "*Method for measuring the rotation of an asymmetric contact lens & lenses for practicing the method*" US Patents 49765333;*1990*
16. Barry L.Atkins et.al; "*Sample indicator lens*" US Patents 6634747;*2003*

17. Donald Morrison et. al; "*Highly visible markings of contact lenses*"; US Patent 5467149;*1995*

18. Jongliang Wu et al; "*Contact lenses bearing identifying marks*" US Patent 6024448; 2000

19. Jongliang Wu et. al; "*Contact lenses bearing marks*" US Patent 6203156;*2001*

20. Akihisa Sugiyama et. al; "*Method of producing contact lens with identifying mark permeating into lens*"; US Patents 5580498;*1996.*

21. Yasuhiro Yokoyama et.al; "*Process for producing contact lens having a mark and contact lens having a mark obtained thereby*"; US Patents 7165840,*2007*

22. David J. Fischer et.al; "*Transparent ophthalmic lens having engraved surface indicia*" US Patents 4194814;*1980*

23. Kazuhiko Nakada et.al; "*Method of marking ophthalmic lens by using laser radiation*" US Patents 6997554;*2006*

24. Schawlow, A.. "*Laser Light*", Scientific American,Vol.219, No.3 (sep 1968),120-136.

25. Coherent,Inc. Staff, Lasers: operation, equipment, application,and design McGraw- Hill,New York, 1980.

26. Ready J. "*Lasers- Their Unusual Properties and Their Influence on Application*", Lasers in Modern Industry, Society of Manufacturing Engineers Marketing Services Dept., Dearborn, MI 1979, 17-38.

27. Eloy, J., Power Lasers, John Wiley, NewYork, 1985.

28. Spalding, I., *"Which Wavelength? – How to Select a Suitable Laser*", Proceeding of the First International Conference on Lasers in Manufacturing, IFS Publications, Ltd., Amsterdam, 1984, 229-234.

29. Laos, O., "*Evaluating a CO2 Industrial Laser System,*" Proceedings of the First Conference on Lasers in Manufacturing, IFS Publications, Ltd., Amsterdam, *1983, 21-30*

30. Humphries, M., H.Kahlert, and K.Pippert, "*The Excimer Laser on its Way to Industrial Applications*", Proceeding of the First Conference on Lasers in Manufacturing, IFS Publications, Ltd., Amstredum, *1983, 255-262.*

31. Weber, H., "*High Power Nd: Lasers for Industrial Applications*", Proceeding of the SPIE-High Power Lasers and Their Industrial Application.Vol.*650 (1986), 92-100*

32. Grigoropoulos, C.P., Bennett, T.D., Ho, J.R., Xu, X.,and Zhang, X., (1996), "*Heat and mass transfer in pulsed-laser-induced phase transformation*," Advances in Heat Transfer, *28, 75-134.*

33. Ivanov, D., and Zhigilei, S. (2003), "*Combined atomistic-continuum modeling of short-pulse laser melting and disintegration of metal films*," Physical Review B, *68, 1-22.*

34. Meijer, J., Du, K., Gillner, A., Hoffmann, D., Kovalenko, V.S., Masuzawa, T., Ostendorf, A.,Poprawe, R., and Schulz, W. (2002), "*Laser machining by short and ultrashort pulses, state of the art and new opportunities in the age of the photons*,"Annals of the CIRP, *51/2, 531-652.*

35. Pronko, P.P. Dutta, S.K., Squier, J., Rudd, J.V., Du,D. and Mourou, G. (1995), "*Machining of sub-micron holes using a femtosecond laser at 800nm*," Optics Communications, 114, 106-110

36. Chichkov, B.N., Momma, C., Nolte, S., von Alvensleben, F., and Tunnermann, A. (1996), "*Femtosecond, picosecond and nanosecond laser ablation of solids*," Applied Physics, A *63, 109-115.*

37. Anil Kurela et al., Review Paper Journal of Biomaterials Applications Vol.20 July, 2005

38. Christel, P., Meunier, A. and Dorlot, J.-M. (1988). "*Biomechanical compatibility and Design of Ceramic Implants for Orthopaedic Surgery*",Ann. N.Y. Acad. Sci., 523: 234–256.

39. Mark J. Jackson et al., Microfabrication and Nanomanufacturing pp.249-250

40. M. R. H. Knowles, "*Micro-machining of metals, ceramics and polymers using nanosecond lasers*", Int J Adv Manuf Technol *(2007) 33:95–102.*

41. Oestendorf A, Kamlage G, Klug F, Chickkov BN (2005) "*Femtosecond versus picosecond laser ablation*". In: Proceedings of the SPIE conference, Photon Processing in Microelectronics and Photonic IV, San Jose, California, January *2005, vol 5713, pp 1–8*

42. Karnakis D, Knowles M, Alty K, Schalf M, Snelling H (2005) "*Comparison of glass processing using high repetition femtosecond (800 nm) and UV (255 nm) nanosecond pulsed lasers*". In: Proceedings of the SPIE conference, Microfluidics, BioMEMS and Medical Microsystems III, San Jose, California, January 2005, vol *5718, pp 216–277*

43. Breitling D, Ruf A, Dausinger F (2004) "*Fundamental aspects in machining of metals with short and ultrashort laser pulses*". In: Proceedings of the SPIE conference, Photon Processing in Microelectronics and Photonic III, San Jose, California, January 2004, vol *5339, pp 49–63*

44. X. Liu, "*Submicon lines in thin metallic films micromachined by an ultrafast laser oscillator*," Technical digest-Conference on Lasers and Electro-Optics *1998, 511 (1998).*

45. http://www.cmxr.com/micromachining/handbook

46. P. P. Pronko, S. K. Dutta, J. Squier, J. V. Rudd, D. Du, G. Mourou, "*Machining of submicron holes using a femtosecond laser at 800nm*," Optics Communications, *114, 106-110 (1995*).

47. Borowiec, H.K. Haugen, "*Morphological and chemical evolution on InP(100)surface irradiated with femtosecond laser*" Appl. Phys. Lett. *82 (2003) 4462.*

48. T.H.R. Crawford, A. Borowiec, H.K. Haugen, CLEO/IQEC and PhAST 2004 Technical Digest on CD-ROM, The Optical Society of America, Washington, DC, 2004, CTuP40.

49. T.Q. Jia, H.X. Chen, M. Huang, F.L. Zhao, J.R. Qiu, R.X. Li, Z.Z. Xu,X.K. He, J. Zhang, H. Kuroda, "*Formation of nanogratings on the surface of a ZnSe crystal irradiated by femtosecond laser pulses*" Phys. Rev. B *72 (2005) 125429.*

50. C.Y. Chien et. al., "*Pulse width effect in ultrafast laser processing of materials*" Appl. Phys. A 81, 1257–1263 (2005).

51. Chen, K. and Yao Y. L. (2000), "*Process optimization in pulsed laser micromachining with applications in medical device manufacturing*," International Journal of Advanced Manufacturing Technology, *16, 243-249.*

52. Bordatchev, E. V. and S. K. Nikumb (2003), "*An experimental study and statistical analysis of the effect of laser pulse energy on the geometric qualityduring laser precision machining*," Machining Science and Technology, *1/1,83- 104.*

53. Ho S.F., and Ngoi, B.K.A. (2004), "*Sub-microdrilling with ultrafast pulse laserInterference*," Applied Physics B, *79, 99-102.*

54. Hariharan "*Basics of interferometry*"

55. W.L. Liang et al.. "*Micromachining of circular ring microstructure by femtosecond laser pulses*" Optics & Laser Technology *35 (2003) 285 – 290.*

56. Kawamura K, Sarukura N, Hirano M, Ito N, Hosono H. "*Periodic nanostructure array in crossed holographic gratings on silica glass by two interfered infrared-femtosecond laser pulses".* Appl Phys Letter *2001;79(9):1228–30.*

57. Kawamura K, Sarukura N, Hirano M, Hosono H. "*Holographic encoding of permanent gratings embedded in diamond by two beam interference of a single femtosecond near-infrared laser pulse".* Japanese J Appl Phys *2000;39:L767–9.*

58. Zhai J, Shen Y, Si J, Qiu J, Hirao K. "*The fabrication of permanent holographic gratings in bulk polymer medium by a femtosecond laser".*J Phys D *001;34:3466-9*

59. Oi K, Barnier F, Obara M. "*Fabrication of fiber Bragg grating by femtosecond laser interferometry".* Proceedings of the Conference of LEOS, San Diego, California, vol. 2, *2001; p. 776–7.*

60. Hideo Hosono et al.. "*Holographic writing of micro-gratings and nanostructures on amorphous SiO2 by near infrared femtosecond pulses*" Nuclear Instruments and Methods in Physics Research B 191 *(2002) 89–97.*

61. Kawamura K, Ogawa T, Sarukura N, Hirano M and Hosono H 2000 "*Fabrication of surface relief gratings on transparent dielectric materials by two-beam holographic method using infrared femtosecond laser pulses*" Appl. Phys. B *71 119–21.*

62. Kawamura K, Sarukura N, Hirano M and Hosono H 2000 "*Holographic encoding of permanent gratings embedded in diamond by two beam interference of a single femtosecond near-infrared laser pulse*" Japan. J. Appl. Phys. *39 L767–9.*

63. K. Venkatakrishnan et. al., "*Direct fabrication of surface-relief grating by interferometric technique using femtosecond laser*" Appl. Phys. A 77, *959–963 (2003)*

64. K. Venkatakrishnan et. Al., "*Fabrication of planar gratings by direct ablation using an ultrashort pulse laser in a common optical path configuration*" Appl. Phys. A *76, 143–146 (2003).*

65. S. Pissadakis et al., "*Ablated gratings on borosilicate glass by 193-nm excimer laser radiation*" Appl. Phys. A 69 [Suppl.], *S739–S741 (1999).*

66. Nissel, G. "*Off-set corneal contact lenses, alias parabolic lenses and suchfike. Ophtha"l.* Optician, *6, 857-860 (1996).*

67. Douthwalte, W.A., Hough, T., Edwards, K. and Notay, H. "*The EyeSys videokeratoscope assessment of apical radius and p-value in the normal human cornea".* Ophthal. Physiol. Opt., *19, 467-474 (1999).*

68. Craig A. Woods, "*MEASURING NON-SPHERICAL OPTICAL SURFACES"* Contact Lens and Anterior Eye *(2001) 24, 9-15.*

69. Henryk T. Kasprzak et al., "*Approximating ocular surfaces by generalized conic curves*" Ophthal. Physiol. Opt. *2006 26: 602–609*

70. Alexander V. Goncharova, Maciej Nowakowski; "*Reconstruction of the Optical System of the Human Eye with Reverse Ray-Tracing"* OPTICS EXPRESS *1692,4 February 2008 / Vol. 16, No. 3*

71. Kiely PM, Smith G, Carney LG. "*The mean shape of the human cornea". Optica Acta 1982; 29:1027–1040.*

72. Mandell RB; "*The enigma of corneal contour*"; Everett Kinsey Lecture. CLAO J *1992; 18:267–273.*

73. Lindsay R, Smith G, Atchison D. "*Descriptors of corneal shape*". Optom Vis Sci *1998; 75:156–158.*

74. Davis WR, Raasch TW, Mitchell GL, et al. "*Corneal asphericity and apical curvature in children: a cross-sectional and longitudinal evaluation*". Invest Ophthalmol Vis Sci *2005; 46:1899–1906.*

75. Jose´ Manuel Gonza´lez-Me´ijome,et al.. "*Asphericity of the anterior human cornea with different corneal diameters*" J Cataract Refract Surg *2007; 33:465–473 Q 2007* ASCRS and ESCRS

76. Yebra-Pimentel E, Gonza´lez-Me´ijome JM, Cervin˜o A, et al. "*Asfericidad corneal en una poblacio´n de adultos jo´venes. Implicaciones cli´nicas*". Arch Soc Esp Oftalmol 2004; *79:385–392*

77. William M. Steen ,Laser material processing,_

78. C.A. Bennett ;Principles of physical optics

79. Werner J. Blau et. al; "*Ablation thresholds in ultrafast laser micro-machining of common metals in air*" Proceedings of SPIE Vol. *4876 (2003)*

80. Narayanswamy R Sivakumar et. al., "*Direct grating writing using femtosecond laser interference fringes formed at the focal point*", J. Opt. A: Pure Appl. Opt. 7 *(2005) 169–174.*

81. http://www.u-oplaz.com/crystals/crystals20-1.htm

82. http://en.wikipedia.org/wiki/Wave_plate.

83. www.klccgo.com/mica.htm

84. www.iit.edu/~smart/acadyear/optics.htm

85. http://en.wikipedia.org/wiki/wollaston prism

86. Eommony D C, Howson R P and Willis L J 1973 "*Laser Mirror damage in germanium at 10.6 μm*" Appl. Phys. Lett. *23 598–600*

87. Guosheng Z, Fauchet P M and Siegman A E 1982 "*Growth of spontaneous periodic surface structures on solids during laser illumination*" Phys. Rev. B 26 *5366–82*

88. B Tan and K Venkatakrishnan; "*A femtosecond laser-induced periodical surface structure on crystalline silicon*" J. Micromech. Microeng. 16 (2006) 1–6

Appendix 1

Average Laser Pulse Power

Power of the laser at different rep rates and diode current:

Ampere	20kHz	30kHz	40kHz	50kHz	60kHz	70kHz	80kHz	90kHz	100kHz
18	1.7	1.8	1.9	1.9	1.9	1.9	2.0	2.0	2.0
19	2.66	2.77	2.92	3.00	3.18	3.19	3.20	3.25	3.28
20	3.0	3.2	3.3	3.35	3.4	3.45	3.5	3.5	3.5
21	4.22	4.5	4.68	4.8	5.00	5.1	5.12	5.3	5.41
22	4.7	4.8	5.1	5.15	5.3	5.33	5.4	5.44	5.5
23	6.02	6.6	6.81	7.0	7.41	7.44	7.55	7.6	7.8
24	6.6	6.9	7.5	7.6	7.7	7.7	7.9	7.9	7.9
25	7.7	8.1	9.30	9.65	9.75	10.00	10.1	10.6	10.70
26	8.3	9.0	10.2	10.25	10.5	10.55	10.7	10.8	10.8
27	9.12	9.5	11.70	12.1	12.50	12.59	12.99	13.21	13.30
28	9.6	10.00	12.5	12.5	13.0	13.1	13.2	13.3	13.4
29	10.34	12.00	13.50	13.70	14.60	14.8	15.12	15.13	15.23
30	10.4	12.1	14.2	14.3	14.9	14.9	15.00	15.15	15.3
31	10.6	12.9	15.00	15.45	16.00	16.05	16.2	16.30	16.4
32	10.8	13.1	15.2	15.5	16.1	16.1	16.3	16.5	16.6

Appendix 2

Experimental Details

(1) Experiments with Different Laser Power:

S.No.	Available Laser Power (watt)	Rep Rate (kHz)	Machining Time (Second)
1	2.321	20	10
2	2.585	,,	,,
3	3.311	,,	,,
4	3.63	,,	,,
5	4.235	,,	,,
6	4.565	,,	,,
7	5.016	,,	,,
8	5.28	,,	,,
9	5.687	,,	,,
10	5.72	,,	,,

(2) Experiments with different rep rates:

S.No.	Available Laser Power (watt)	Rep Rate (kHz)	Machining Time (Second)
1	3.63	20	5
2	,,	30	,,
3	,,	40	,,

(3) Experiments with different focusing lens:

S.No.	Focusing Length (mm)	Rep Rate (kHz)	Machining Time (Second)
1	100	20	10
2	50.8	,,	,,
3	25.4	,,	,,

(4) Experiments with different beam spacing:

S.No.	Beam Spacing (mm)	Rep Rate (kHz)	Machining Time (Second)
1	12	20	10
2	9	,,	,,
3	6	,,	,,

Appendix 3

MATLAB Coding

```
clear all;
clc;
 i=1;
   wavelength = 1.064;
   b=2300;
   po=input('Enter the value of average power from the laser head without any losses=');%As power after head is 7.7watt at 20kHz and efficiecy of the setup for -200 diverging
   R=20000;%input('Enter the value of Rep Rate=');
   Z=13000;
   y=0;
   f=100000;
   wb=b/2;
   ss=2.44*(wavelength)*(f/b);
   ws=ss/2;

   A=(b)*(ss)*(10^-4)^2;
   E=po/R;
   Io=(0.5*E/A)*0.34*0.55;%Multiplied with 0.34 as absorption of stainless steel is 40,multiplied with 0.55 for the efficiency of transmission of system%

   for x=-ss:0.01:ss

      PD=(x*Z)/f;
      delta(i)=(2*pi*PD)/wavelength;
      mm(i)=(cos(delta(i)/2))^2;

       %I(i)=4*Io*mm(i)*exp(-2*x^2/wo^2);
       I(i)=4*Io*mm(i)*exp(-((x^2/ws^2)+(y^2/wb^2)));
      dd(i)=x;
      i=i+1;
   end
   plot(dd,I,'r')
   hold on
   title('Machined Spot Size With Respect to Full Width Half Maximum ')
   xlabel('Machined Region')
   ylabel('Single Pulse Intensity in J/cm2')


yy=0.16;
plot(dd,yy)
```